Status of the EXO double beta decay project

Russell Neilson
Stanford University

Outline

- Introduction to double beta decay
- Brief overview of EXO activities
- EXO-200
    - EXO-200 systems
    - Recent milestones and current status

Double beta decay

Extremely rare nuclear decay where two neutrons decay into two protons simultaneously.

$(A,Z) \rightarrow (A,Z+2) + 2e^{-} (+2\overline{\nu}_e)$

Only observable when single beta decay is energetically forbidden.

Double Beta Decay has been observed for a handful isotopes, although not for ^{136}Xe.

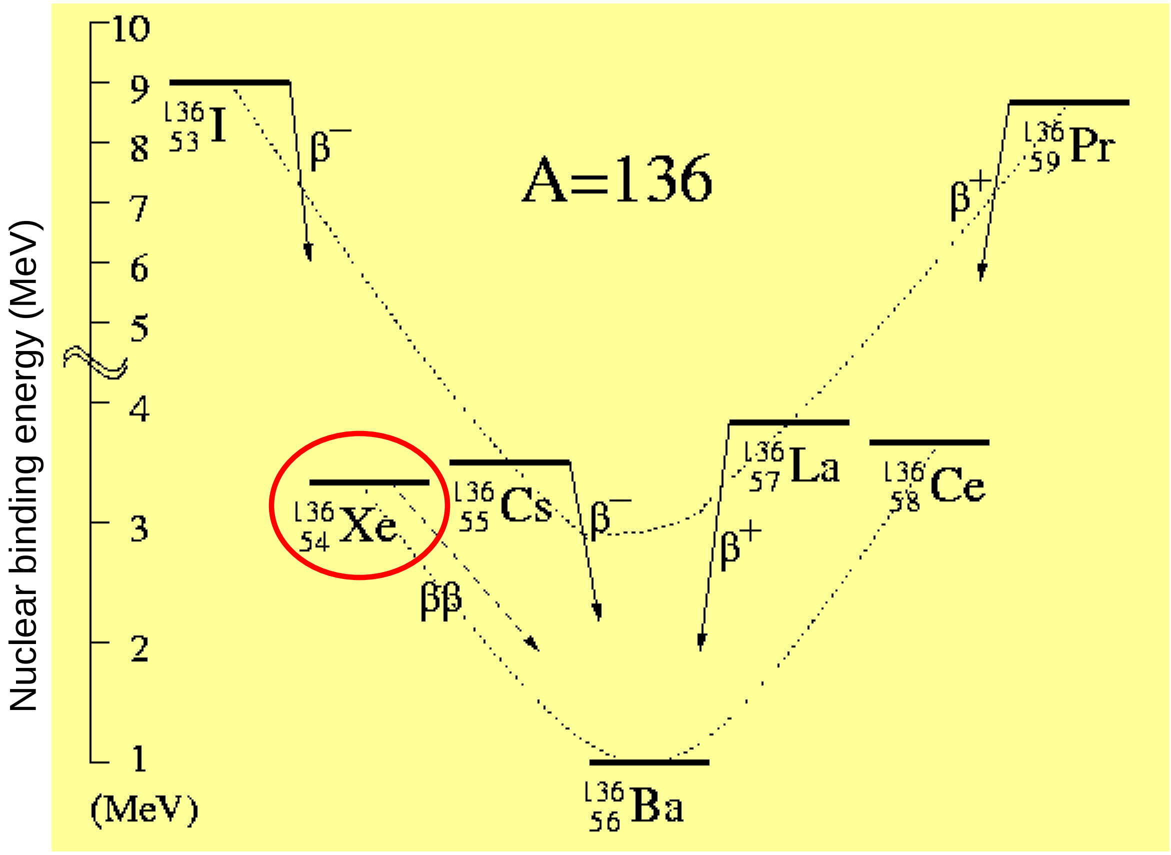

Two types of double beta decay

Two neutrino double beta decay

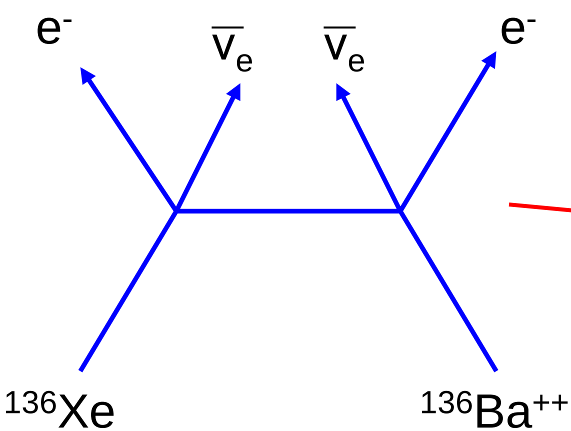

Neutrinoless double beta decay

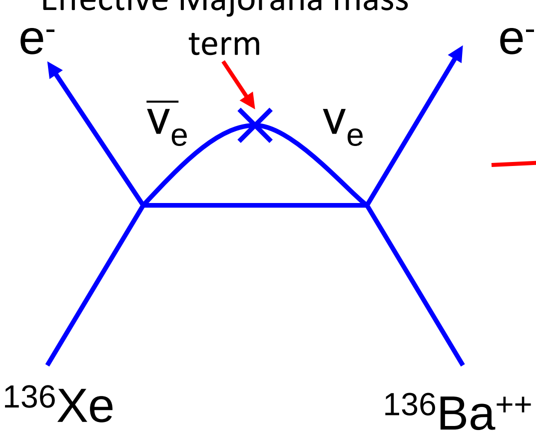

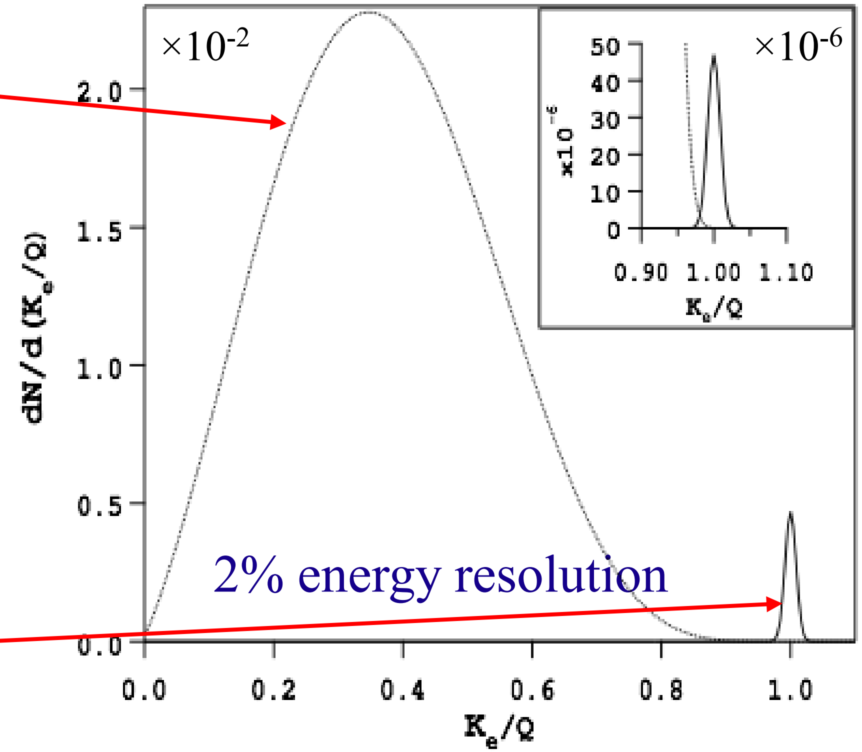

[P. Vogel, arXiv:hep-ph/0611243]

Neutrino masses

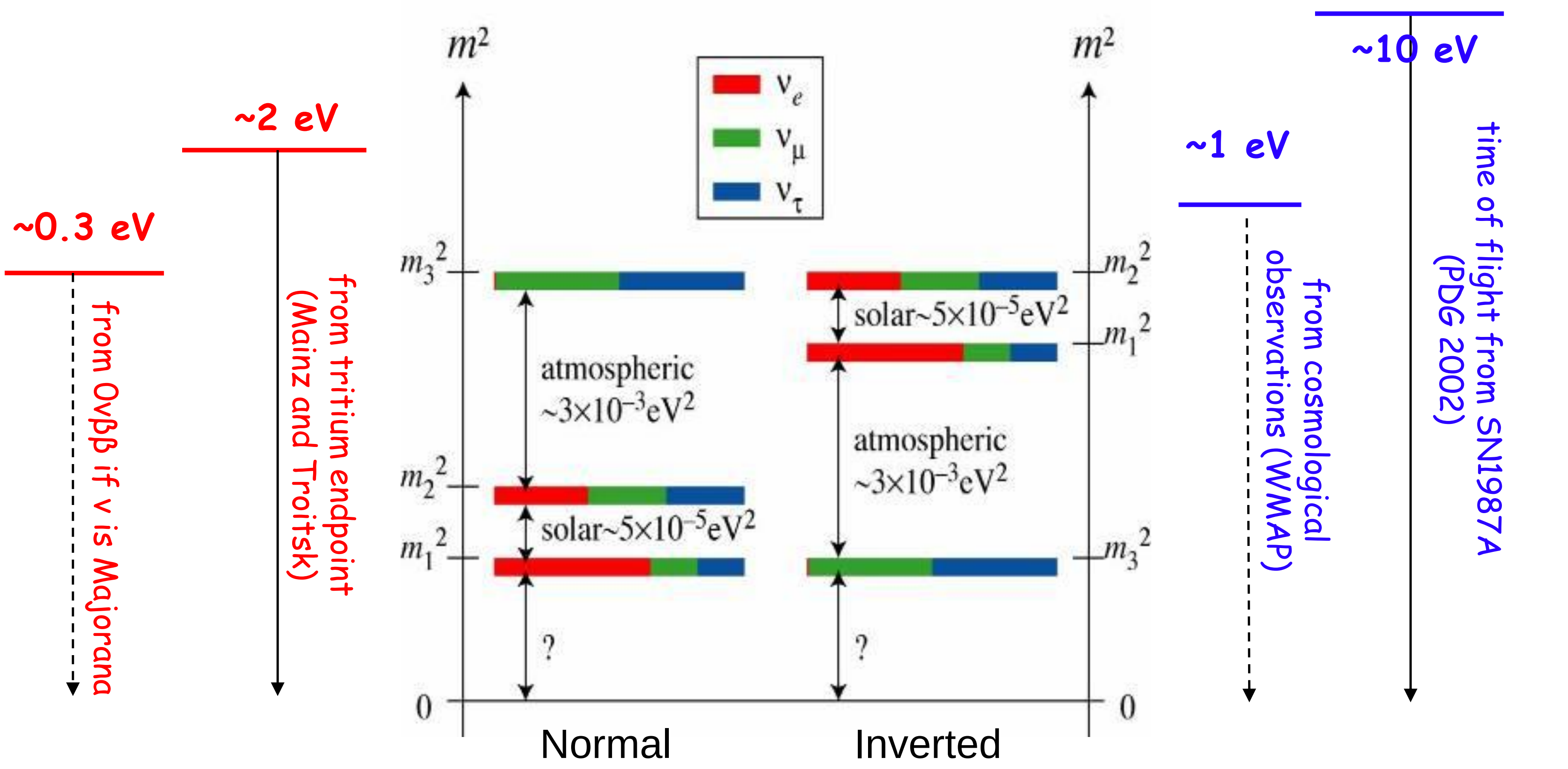

Neutrinoless double beta decay

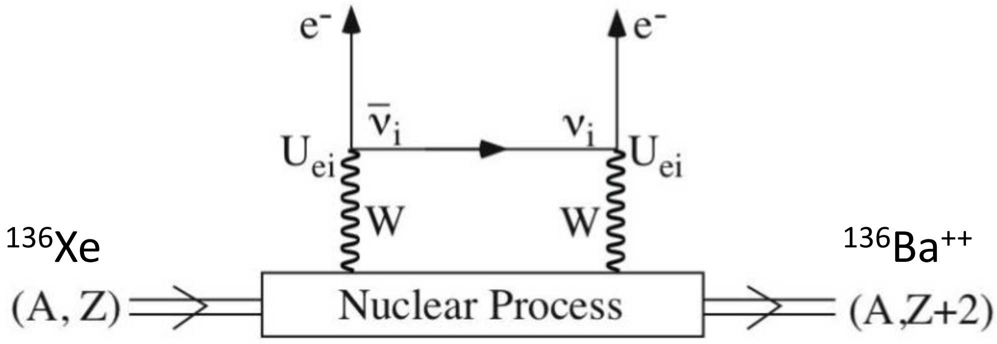

$$\left|\sum_i m_i U_{ei}^2\right| \equiv \left|\langle m_{\beta\beta}\rangle\right|$$ Effective Majorana mass is a coherent sum over mass eigenstates

$$\left(T_{1/2}^{0\nu\beta\beta}\right)^{-1} = G_{0\nu\beta\beta}\left(Q_{\beta\beta}, Z\right)\left|M_{0\nu\beta\beta}\right|^2 \langle m_{\beta\beta}\rangle^2$$ Decay rate observed in a detector

$0\nu\beta\beta$ requires that neutrinos are massive Majorana particles, and lepton number non-conservation

$$\boxed{\bar{\nu}_i = \nu_i \qquad m_\nu \neq 0 \qquad \Delta L \neq 0}$$

Probing the ν hierarchy with 0νββ

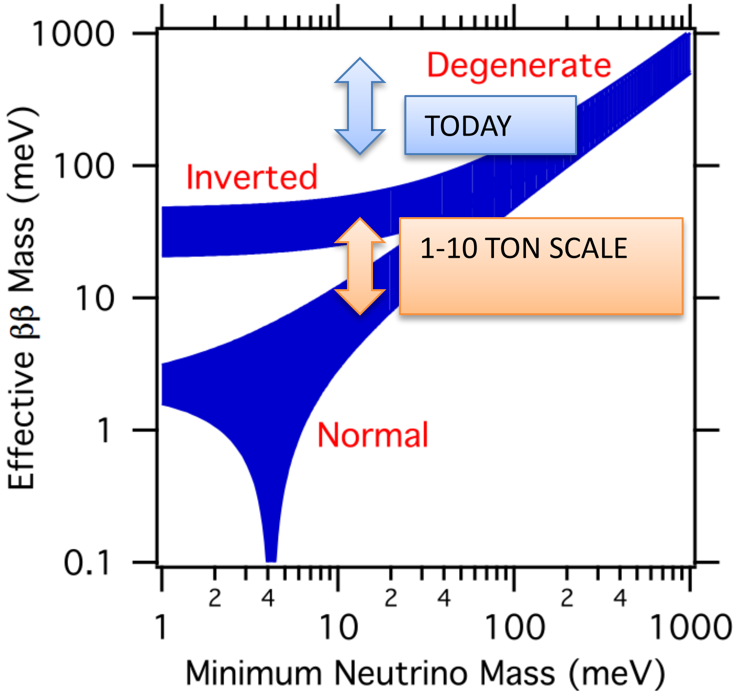

Avignone, Elliot, Engel arxiv:0708.1033 (2007)

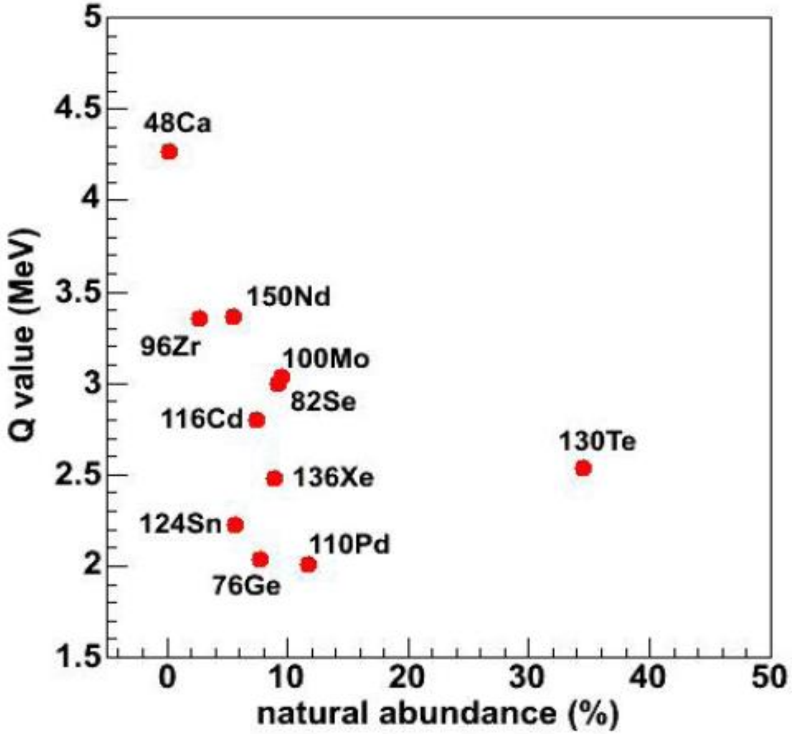

EXO-200 probes the 100 meV scale
Full EXO (1-10 ton) probes 33-5 meV scale

Why use xenon?

Xenon isotopic enrichment is easier. Xenon is a gas & ^{136}Xe is the heaviest isotope.

Xenon is "reusable". Can be repurified & recycled into new detector.

Monolithic detector. LXe is self shielding, surface contamination minimized.

Minimal cosmogenic activation. No long lived radioactive isotopes of xenon.

Energy resolution in LXe can be improved. Scintillation light/ionization correlation.

… admits a novel coincidence technique. Background reduction by barium daughter tagging.

The EXO concept

Measure energy and position of decay event in a Time Projection Chamber (TPC)

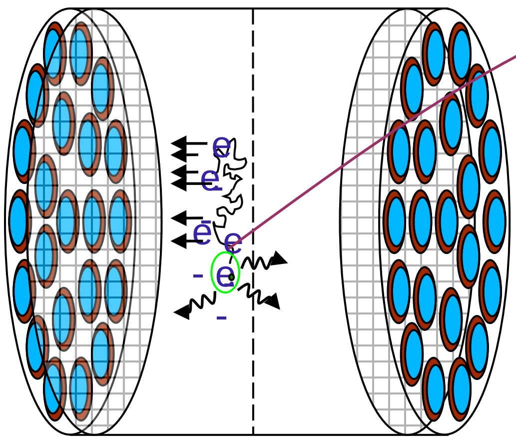

Transfer Ba^+ to an RF trap with a probe

Identify the barium ions with laser spectroscopy

Detect flourescence light with a CCD

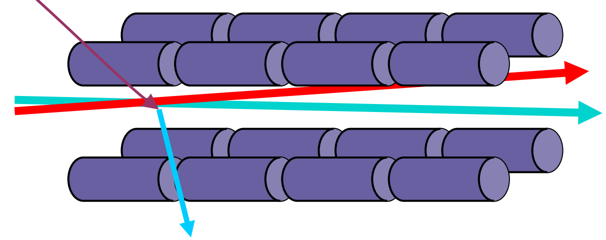

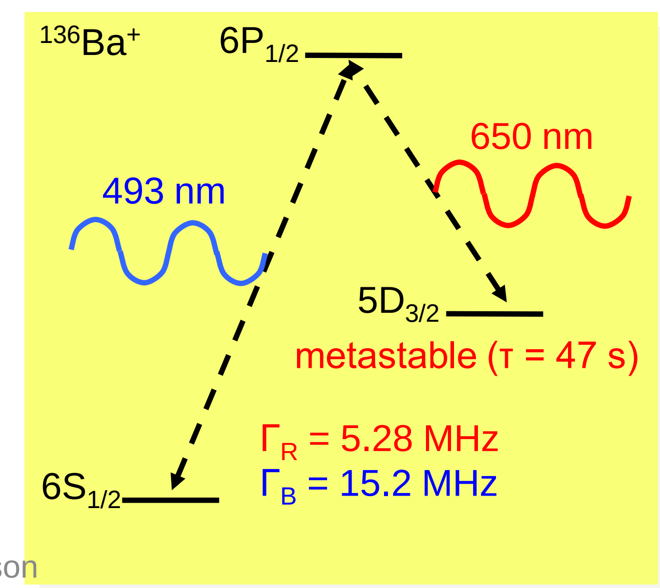

EXO-200

A 200kg enriched liquid xenon low-background TPC with simultaneous ionization and scintillation read-out.

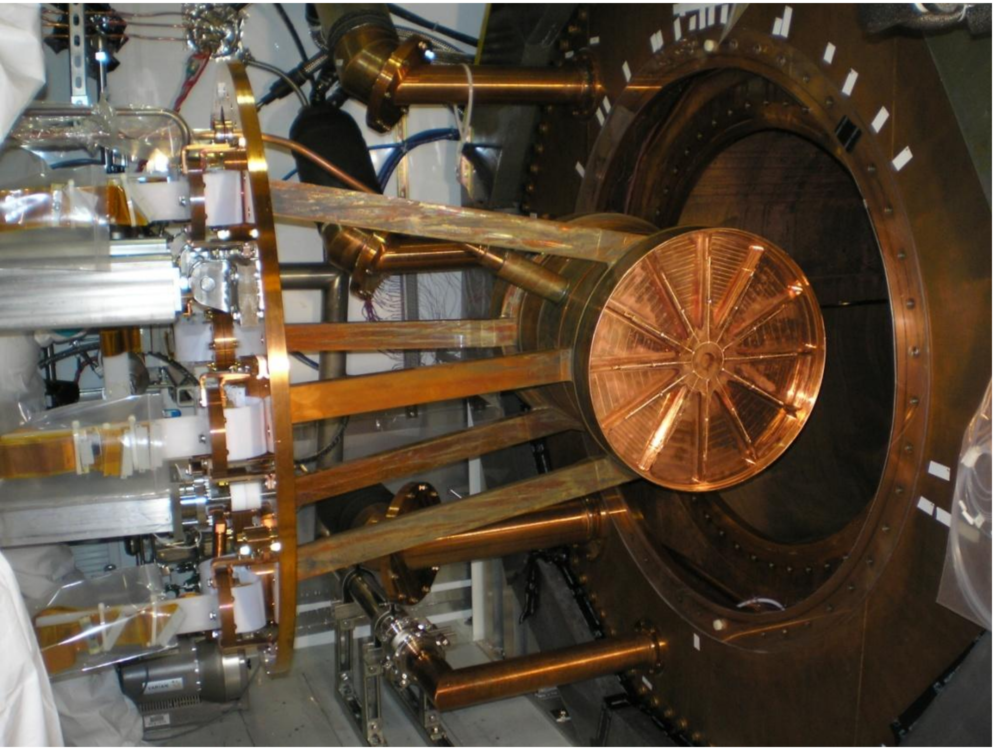

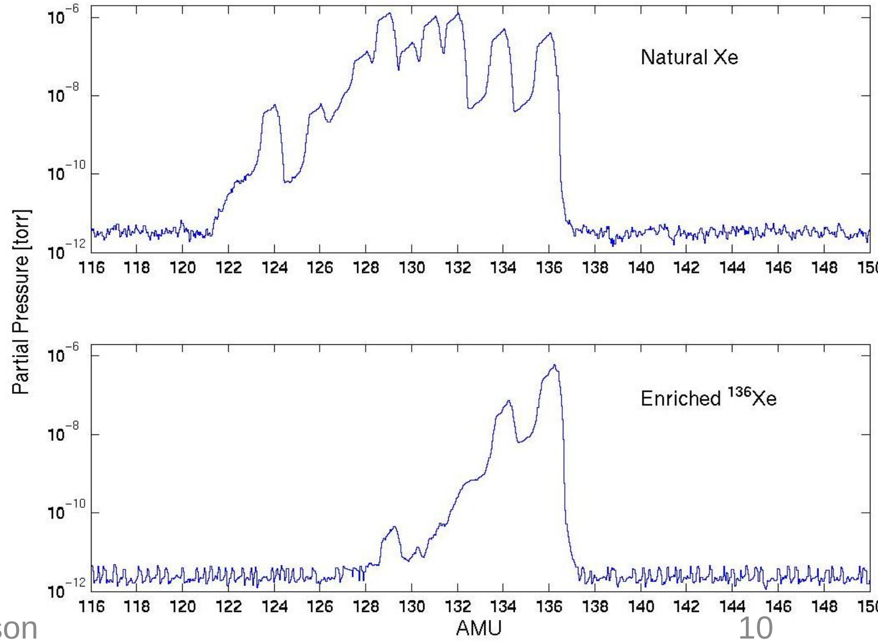

Gas xenon prototype under construction

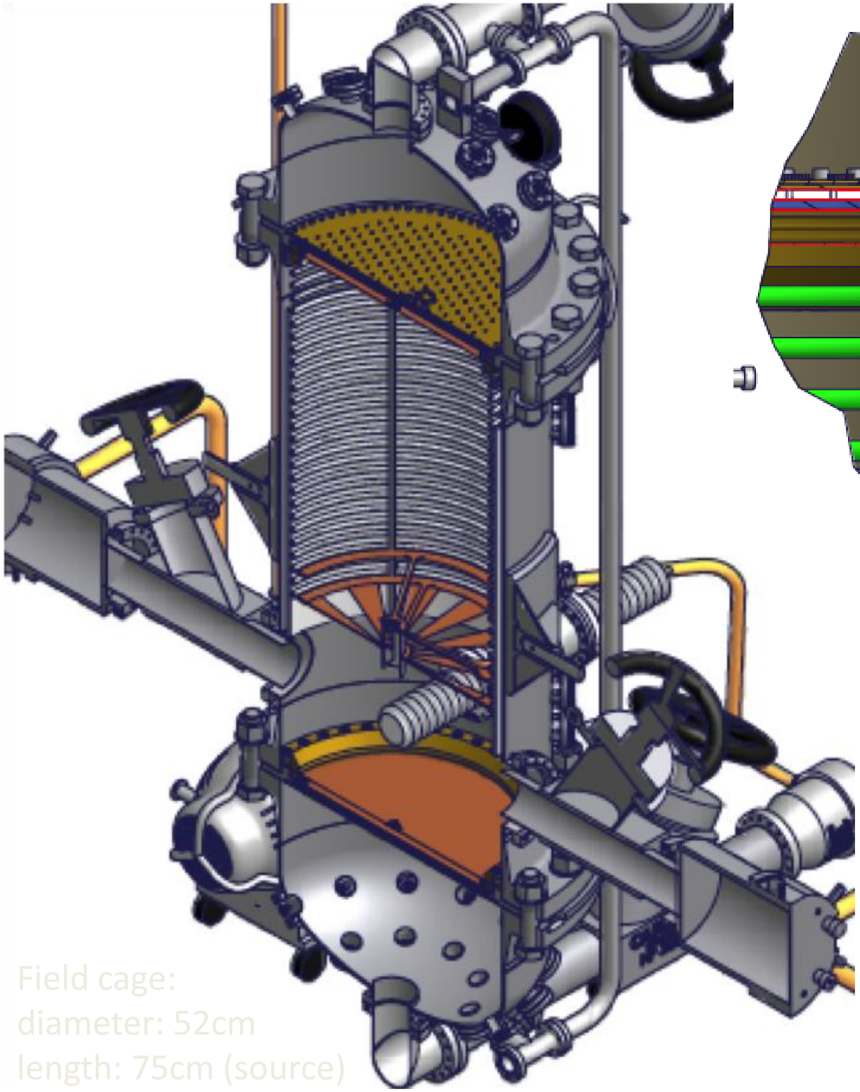

Field cage:
diameter: 52cm
length: 75cm (source)

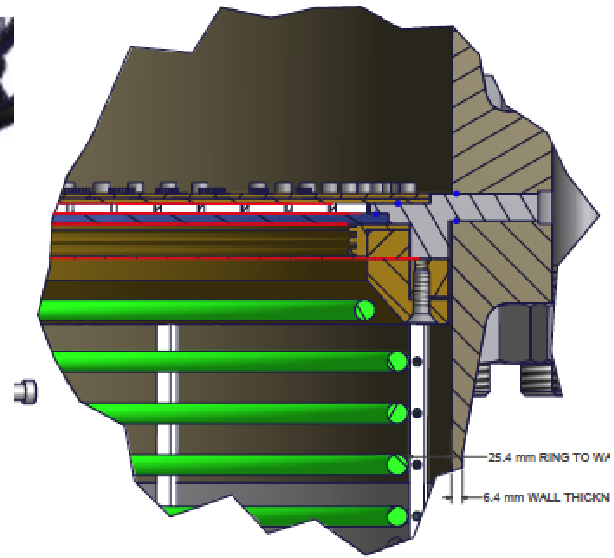

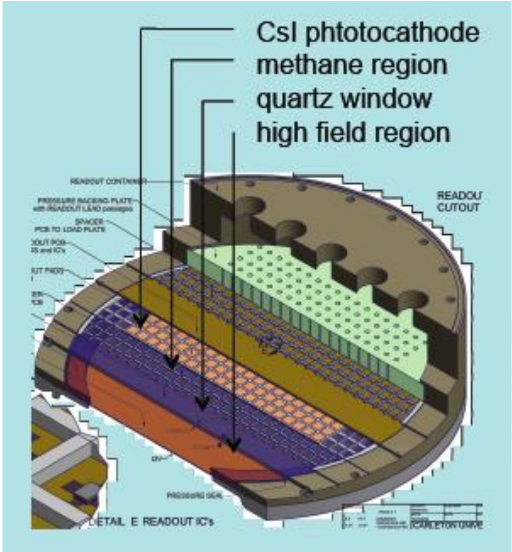

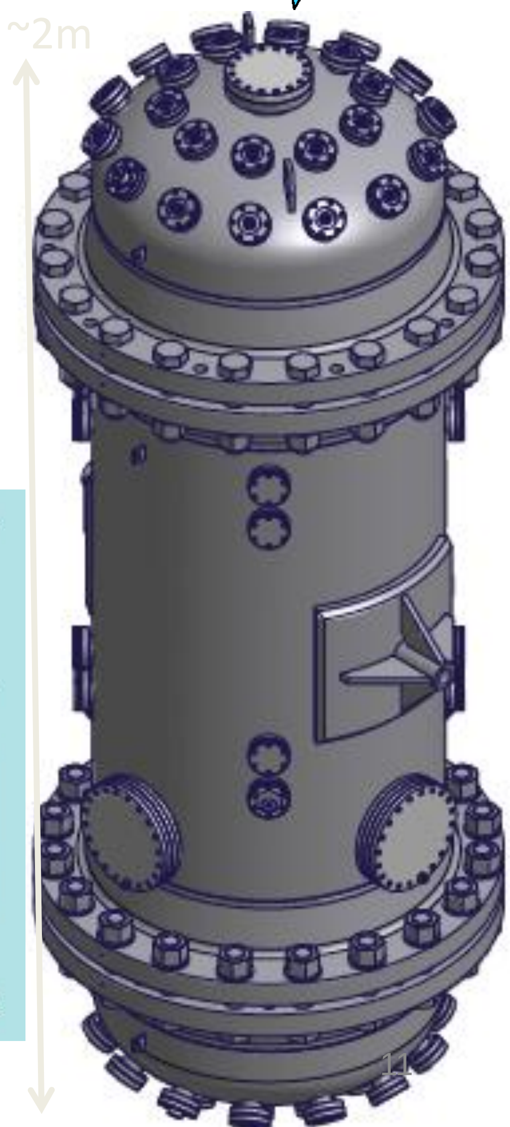

Ba^+ in a gas-filled quadrupole ion trap

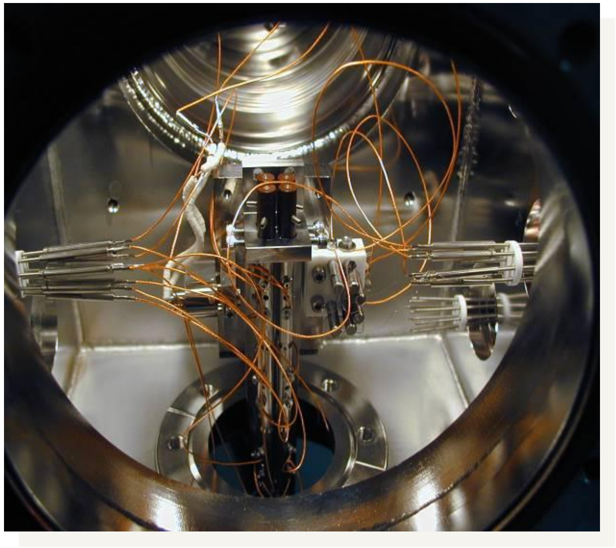

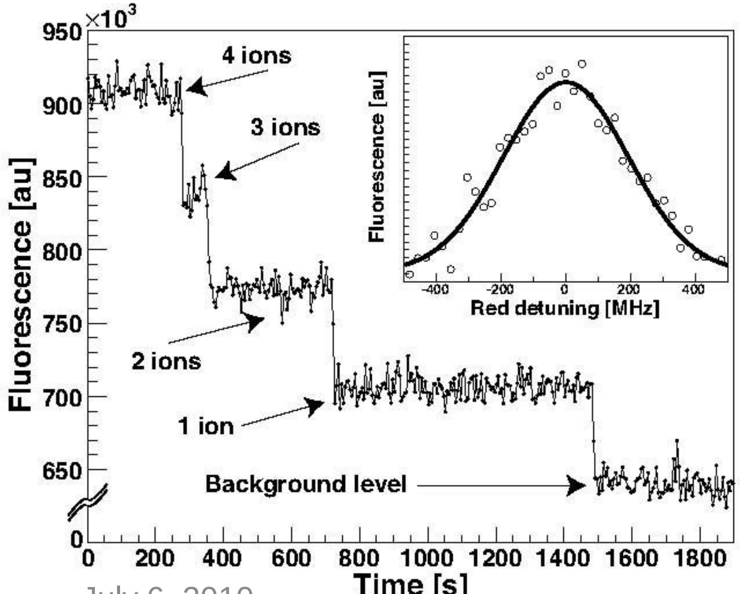

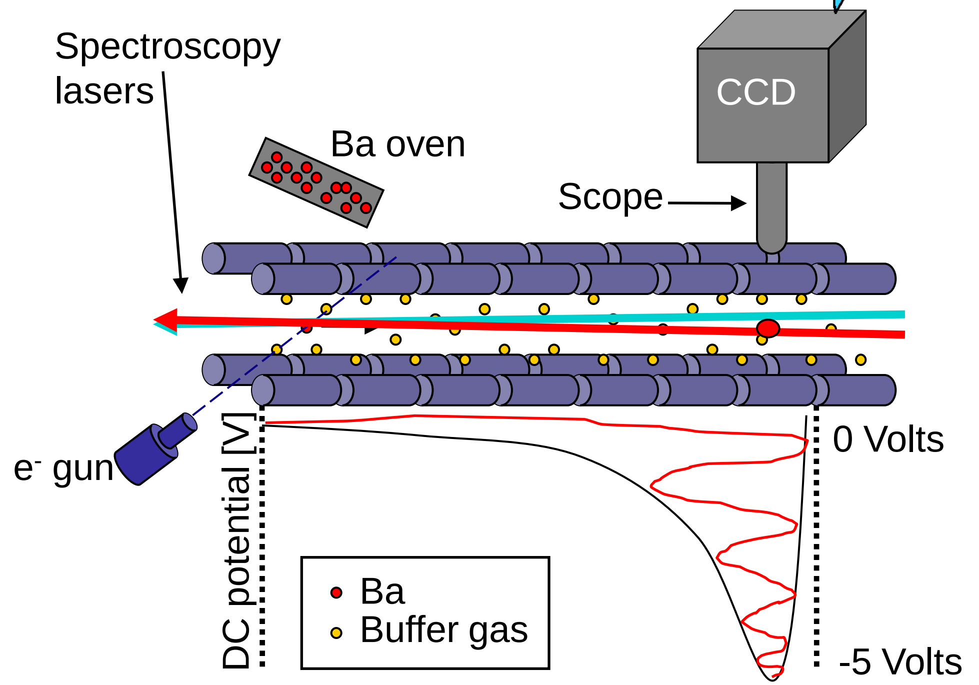

- Observed fluorescence of a single Ba^+ in a buffer gas filled ion trap (~ 10^{-3} torr He, some Xe)

M.Green et al., Phys Rev A 76 (2007) 023404
B.Flatt et al., NIM A 578 (2007) 409

Resonant Ionization spectroscopy (RIS)

- RIS uses lasers tuned to atomic resonances to first *excite* and then *ionize* neutral Ba.
- Pulsed dye lasers at 553.5 nm and 389.7 nm
- Ions counted in a channeltron
- Plan: couple RIS system to quadrupole ion trap

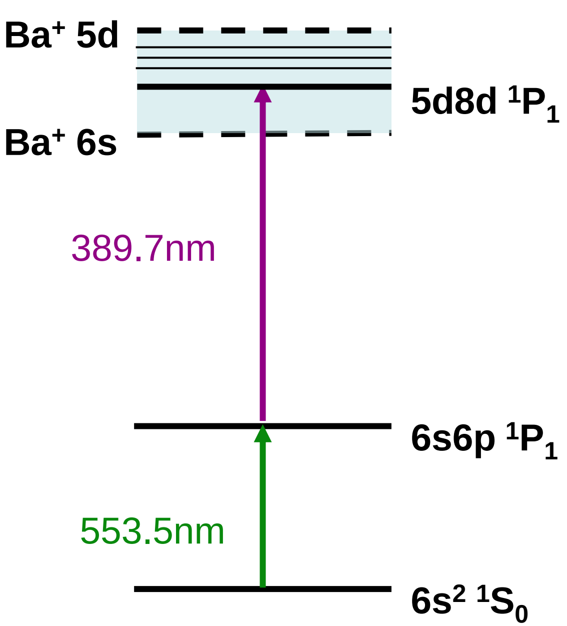

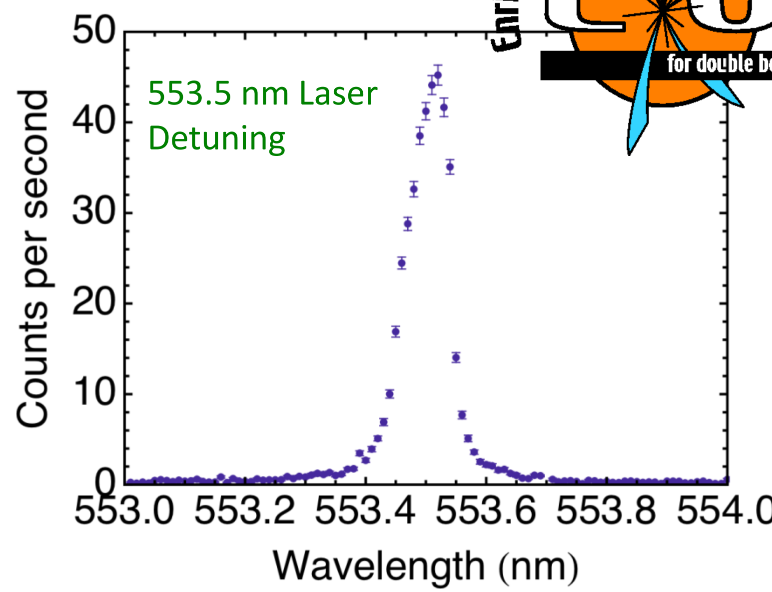

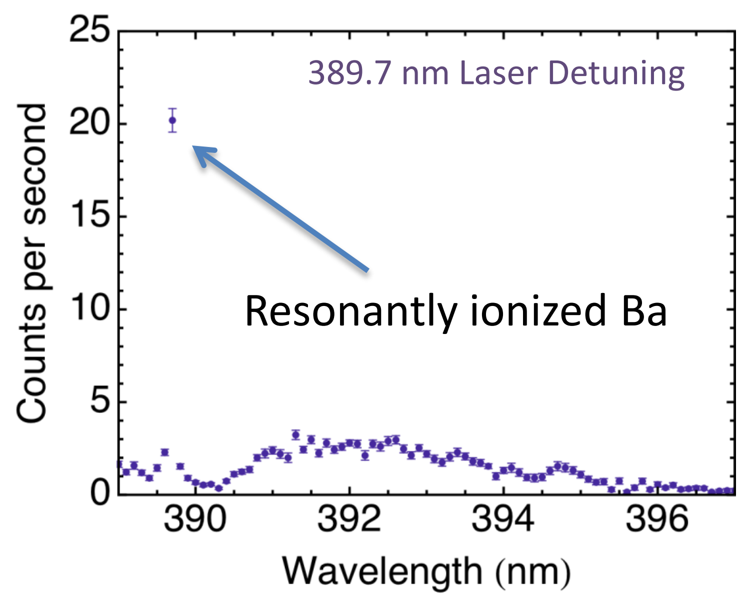

RIS time of flight

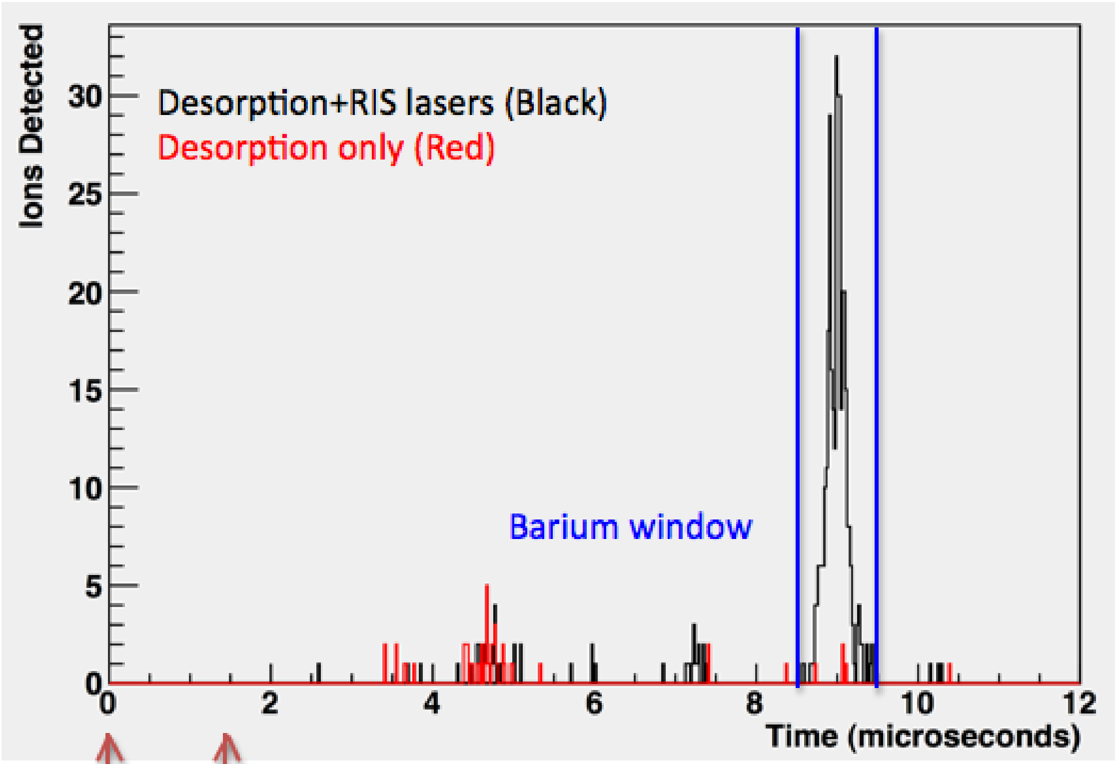

Desorption laser fires

RIS lasers fire

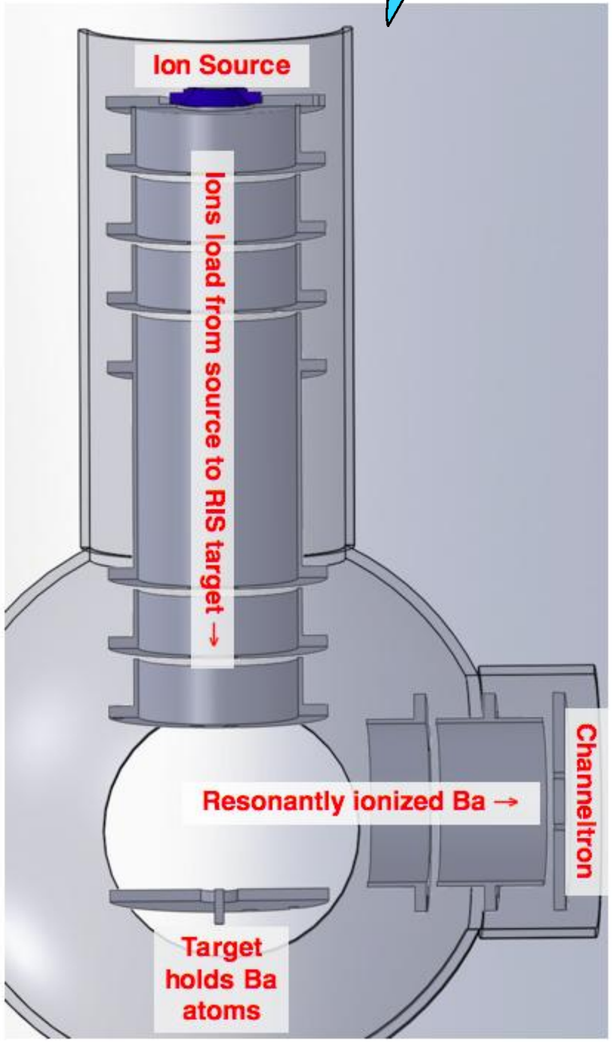

Efficiency of ~10^{-3} in "bulk mode" setup. New "single ion mode" setup being tested now.

Single barium ion source

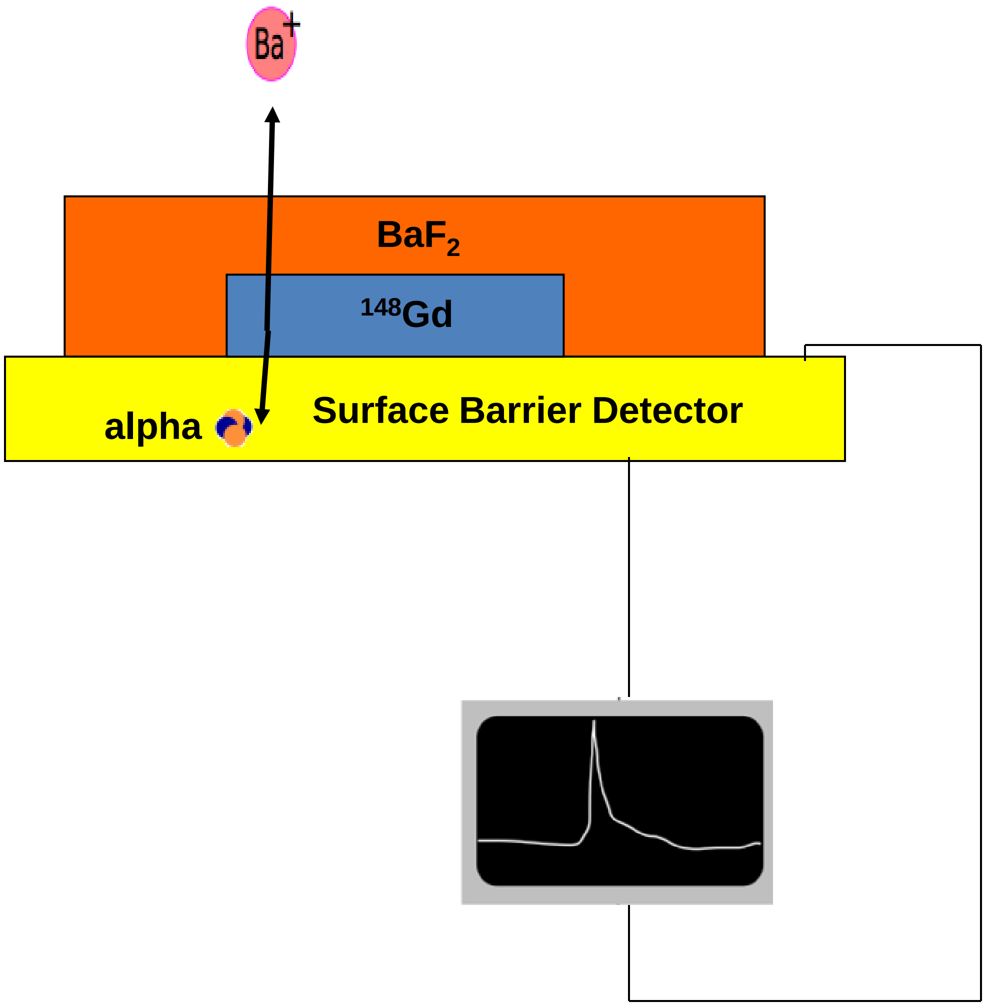

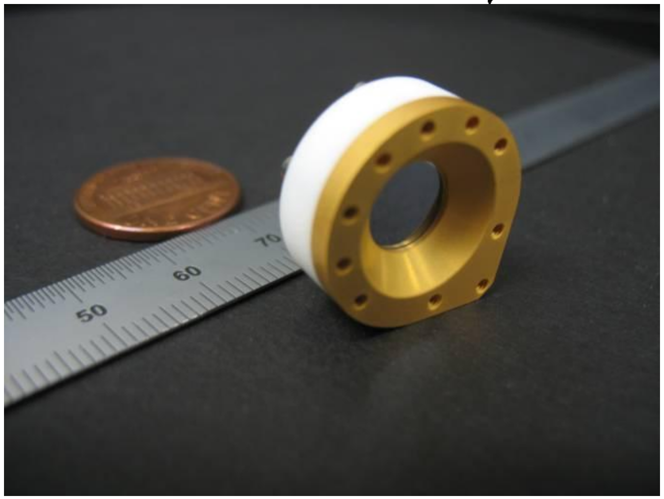

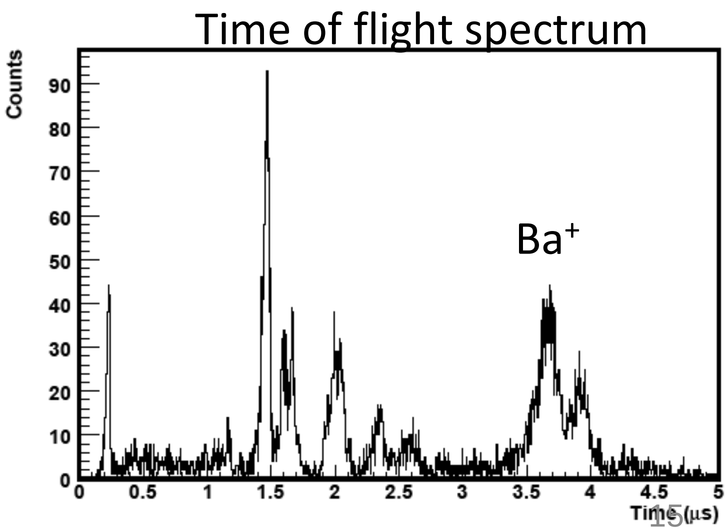

EXO-200 TPC

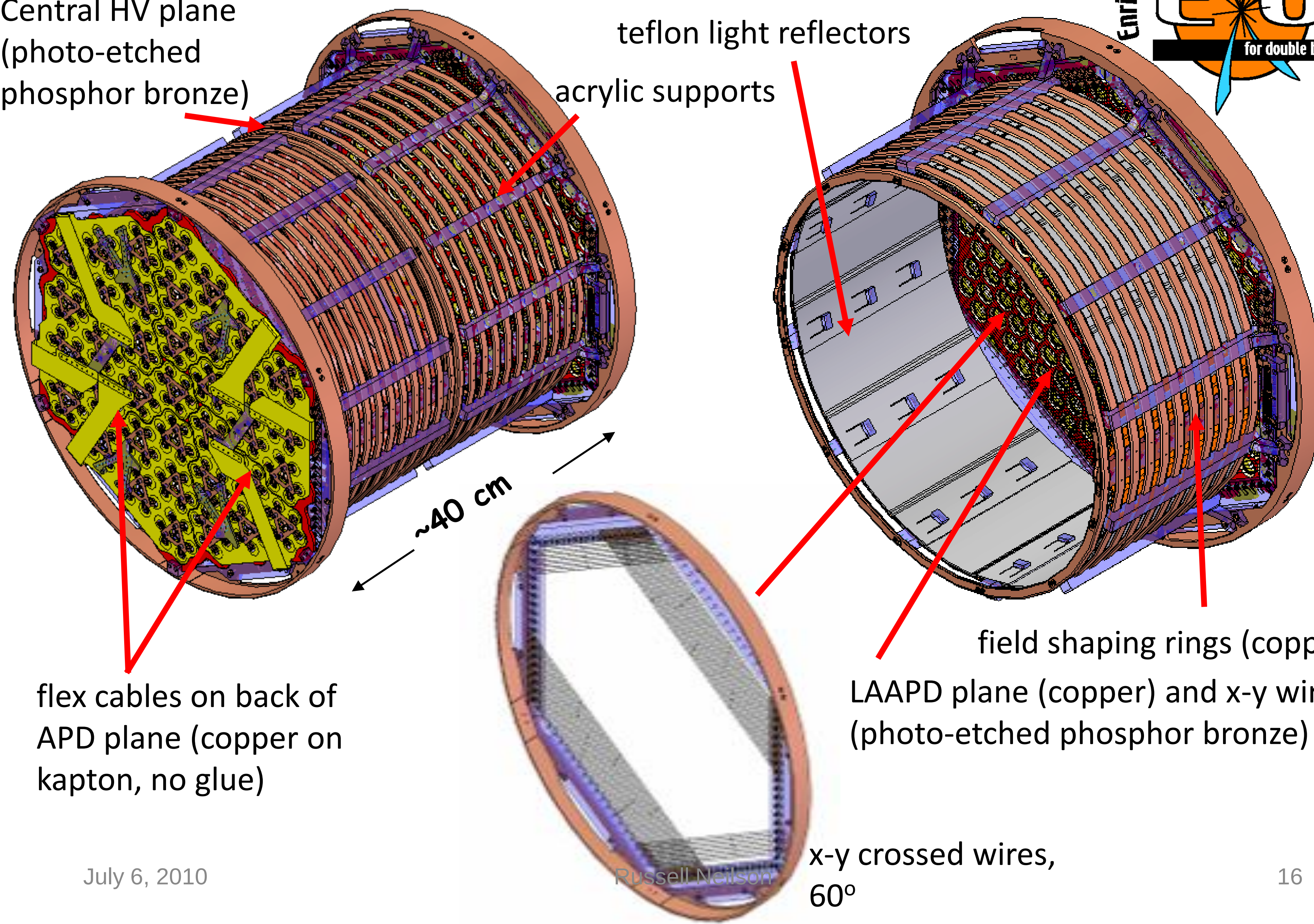
Central HV plane (photo-etched phosphor bronze)
teflon light reflectors
acrylic supports
~40 cm
flex cables on back of APD plane (copper on kapton, no glue)
field shaping rings (copper)
LAAPD plane (copper) and x-y wires (photo-etched phosphor bronze)
x-y crossed wires, 60°

EXO-200 cryostat and lead shielding

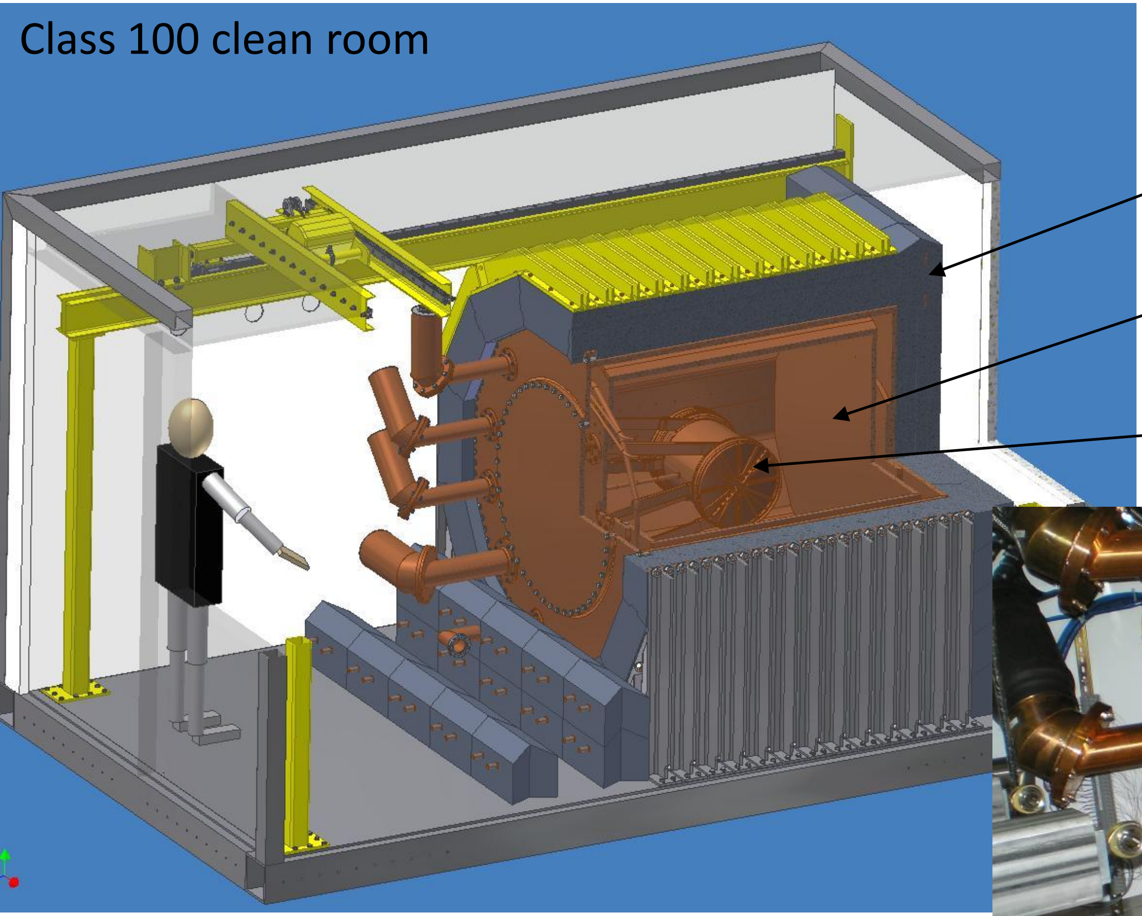

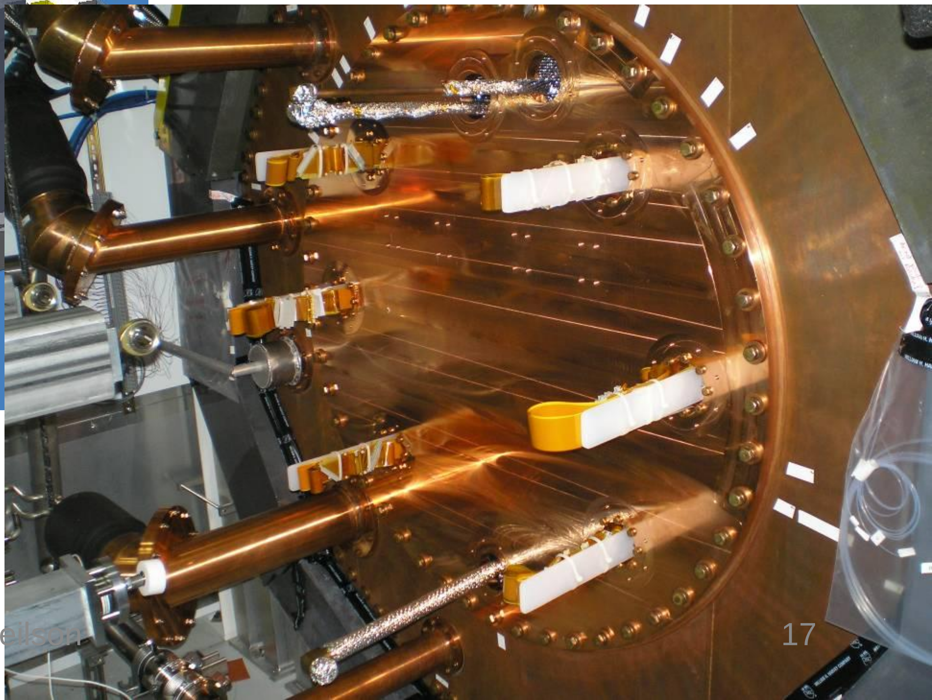

WIPP underground facility

EXO-200 has been assembled and commissioned at Stanford, and transported to WIPP in Carlsbad, NM.

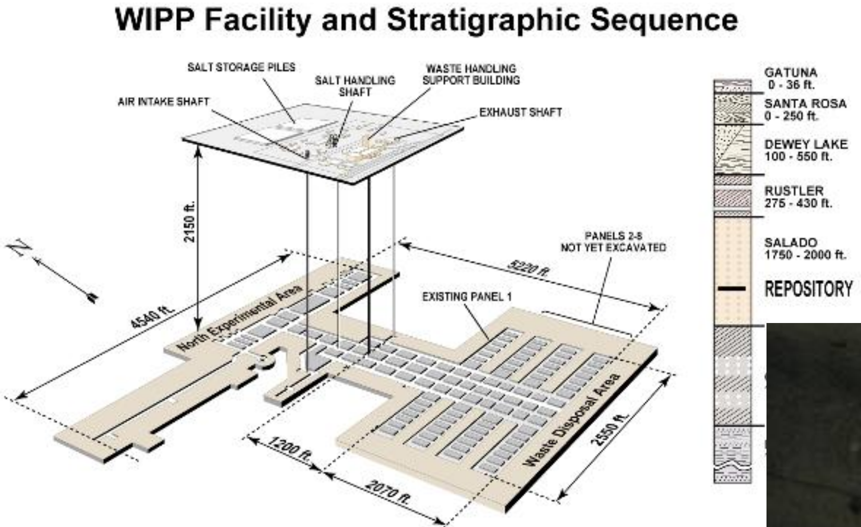

1600m water equivalent depth

Materials qualification database

- Neutron Activation Analysis (NAA) - Alabama (MIT reactor)
- ICP-MS and GD-MS - INMS (Ottawa), commercial outfits
- Radon emanation - Laurentian (Sudbury)
- Gamma counting - Neuchâtel, Alabama
- Alpha counting - Alabama, Carleton, SLAC, Stanford
- Monte Carlo

EXO materials testing summary

Material	Information Source	MD#	K conc. [10^{-9} g/g]	Th conc. [10^{-12} g/g]	U conc. [10^{-12} g/g]
TPC and Internals					
SNO acrylic, batch 48, panel 09.	UA, NAA 8/26/06	59	<3.1	<16	<22
Dupont Vespel, batch SP-1 PLAQUE PGF 9713. Plaque 1. EXO production 6/22/06. Material reserved at Dupont.	UA, NAA 8/26/06	74.1	282±29	<12	<18
Dupont Vespel, batch SP-1 PLAQUE PGF 9714. Plaque 2. EXO production 6/22/06. Material reserved at Dupont.	UA, NAA 8/26/06	74.2	62±7	<25	<28
Norddeutsche Affinerie OFRP copper. Produced 6/1/2006 for EXO. Batch E263/3E1. Sample DOWN collected at DESY.	INMS (Canada) ICPMS 9/1/06	85	<55	<0.5	<0.3
Norddeutsche Affinerie OFRP copper. Produced 6/1/2006 for EXO. Batch E263/3E1. Sample UP2 collected at DESY.	INMS (Canada) ICPMS 9/1/06	85	<50	<0.5	<0.3
	INMS				

D. Leonard et al., Nucl. Inst. Meth. A 591 (2008) 3.

LAAPDs for scintillation light detection

- Low intrinsic radioactive contamination.
  - Lightweight (0.5g each)
  - Made from high purity silicon
  - Fabricated in clean room environments
  - High purity aluminum supplied to manufacturer
- High quantum efficiency for 175nm light (>50%).
- Small physical size.

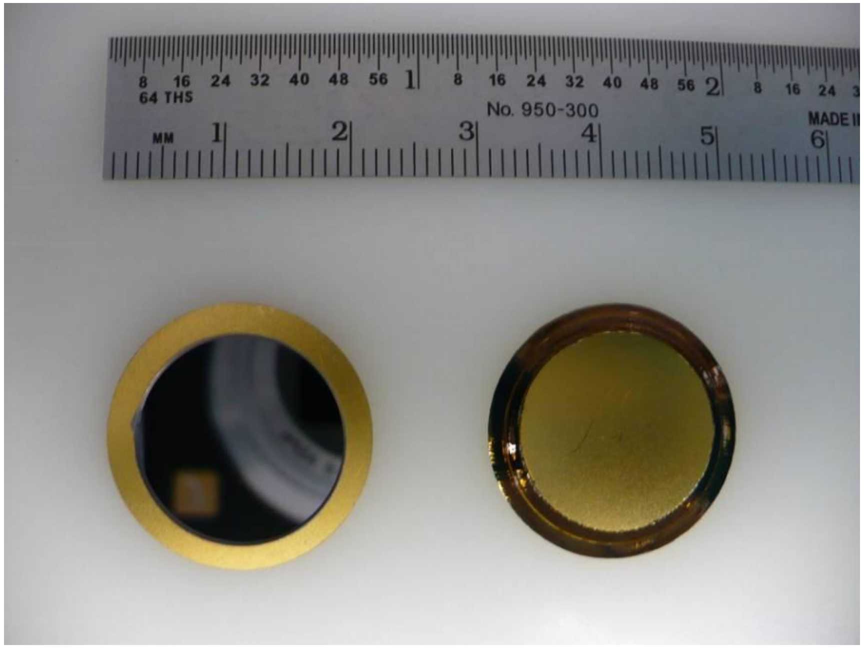

LAAPD properties – leakage current

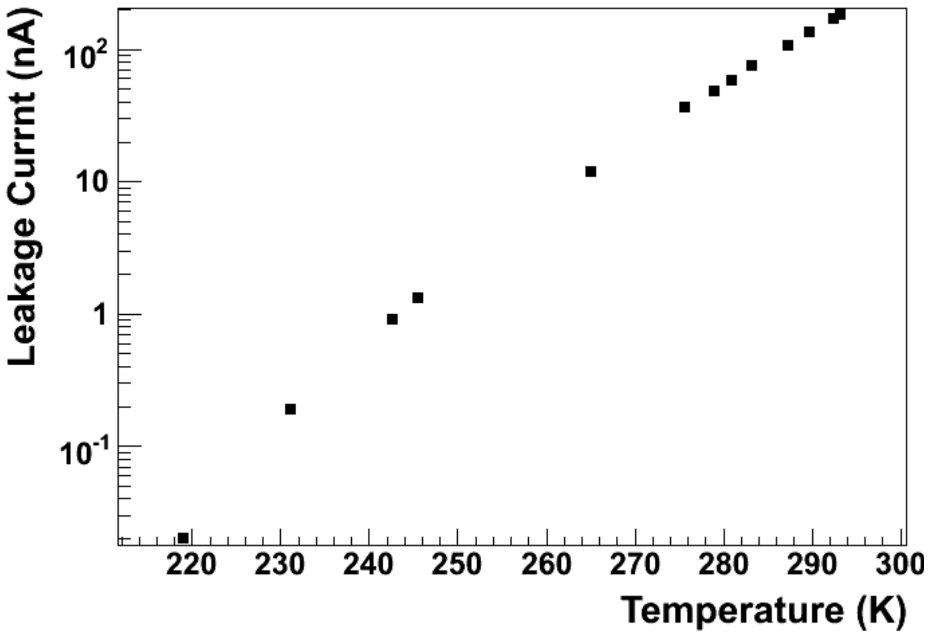

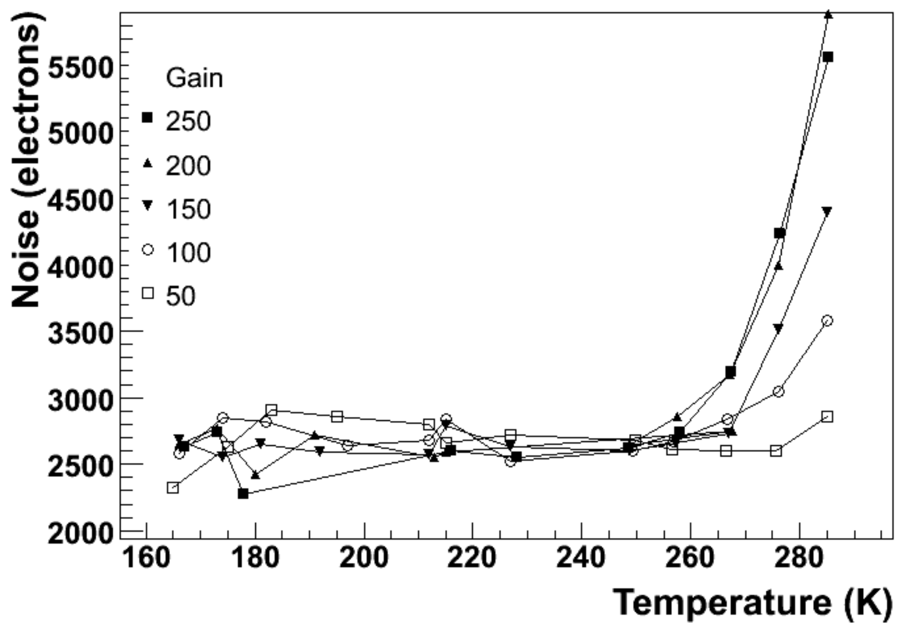

Leakage current drops by over 4 orders of magnitude from room temperature to liquid xenon temperature (169K).

Electronic noise decreases with leakage current

LAAPD properties - gain

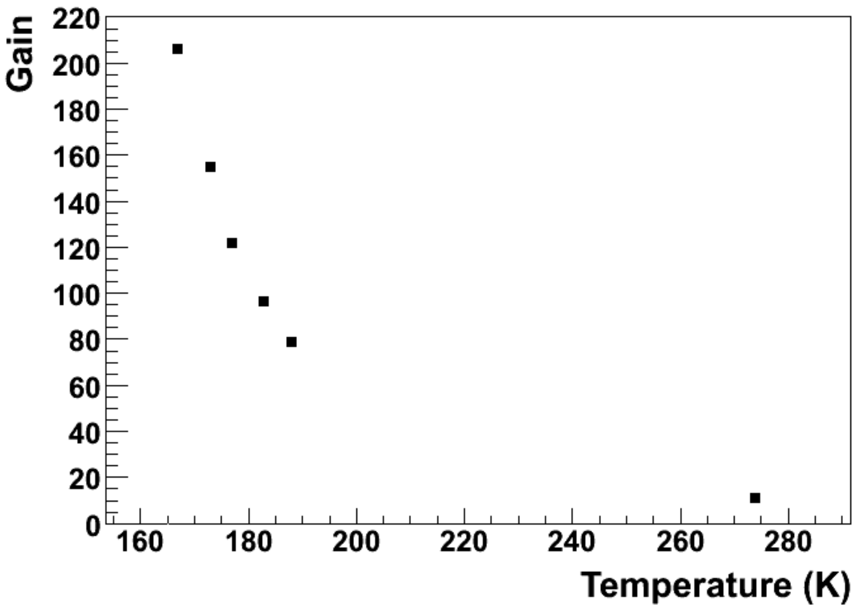

At 169K, gain changes by 5% K^{-1}

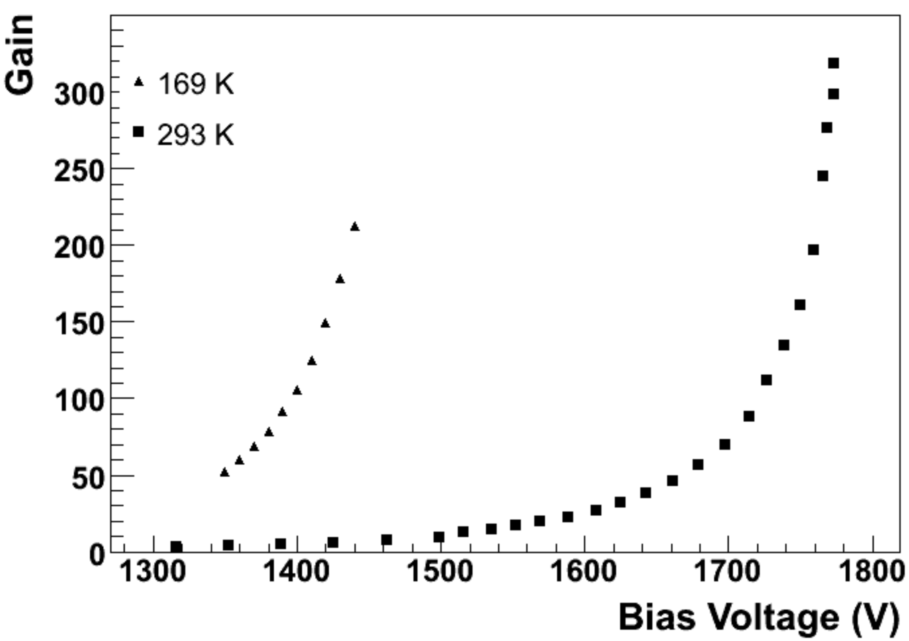

Gain increases by 1.5% V^{-1}

LAAPD characterization

468 LAAPDs are used in EXO-200. They were tested 16 at a time in the APD testing chamber.

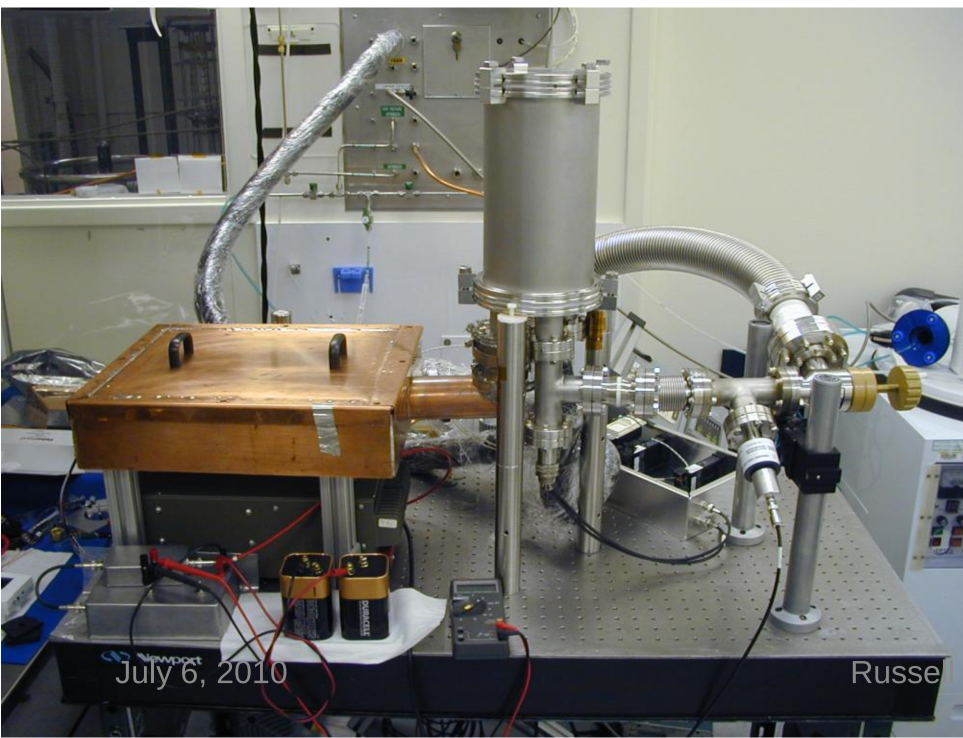

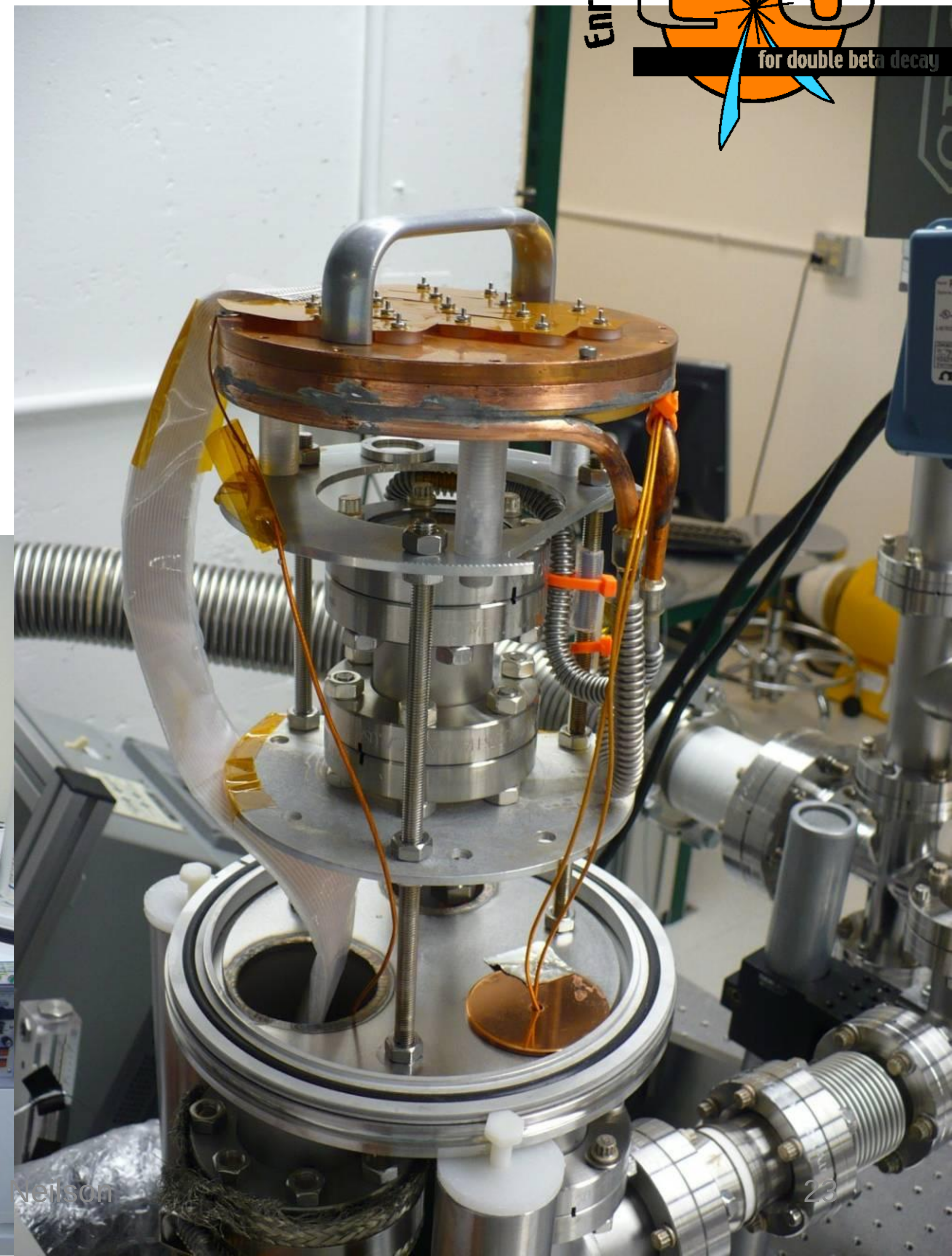

LAAPD test chamber

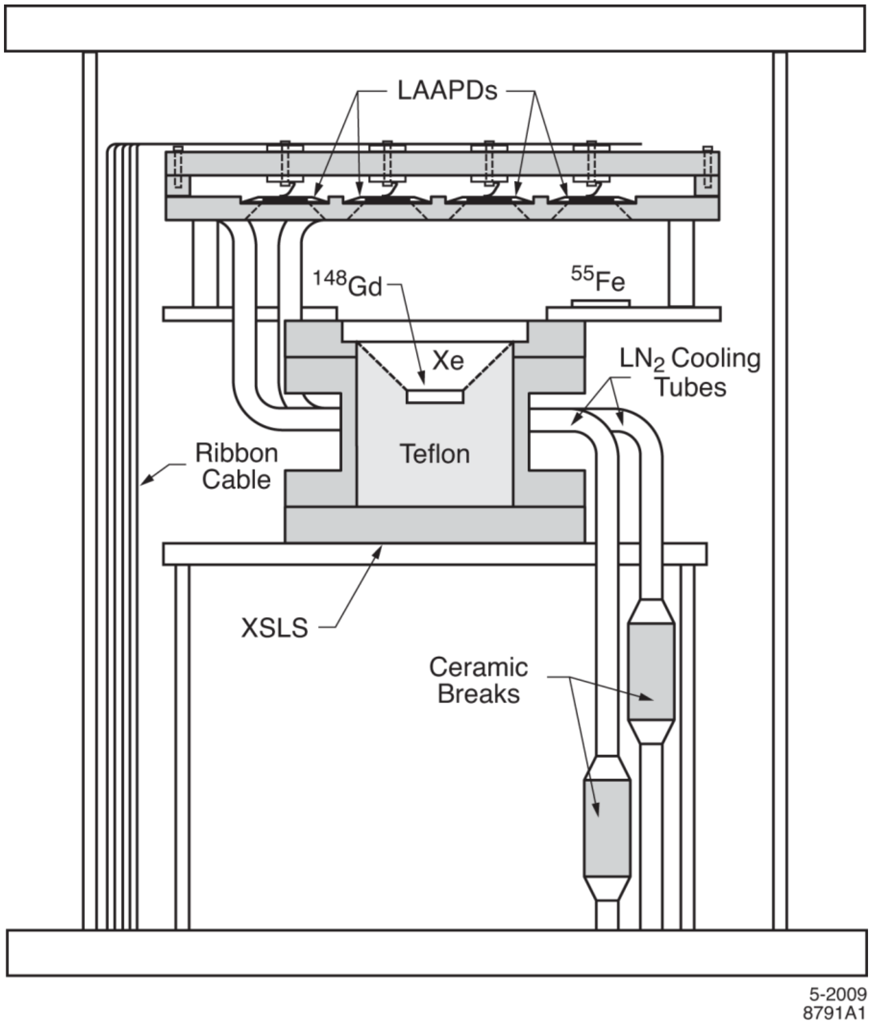

Two radioactive sources:

• ^{55}Fe – mono-energetic 5.9 keV X-rays for measuring APD gain.

• Xenon Scintillation Light Source– alpha source in xenon gas for measuring QE at 175nm.

Test chamber cooling

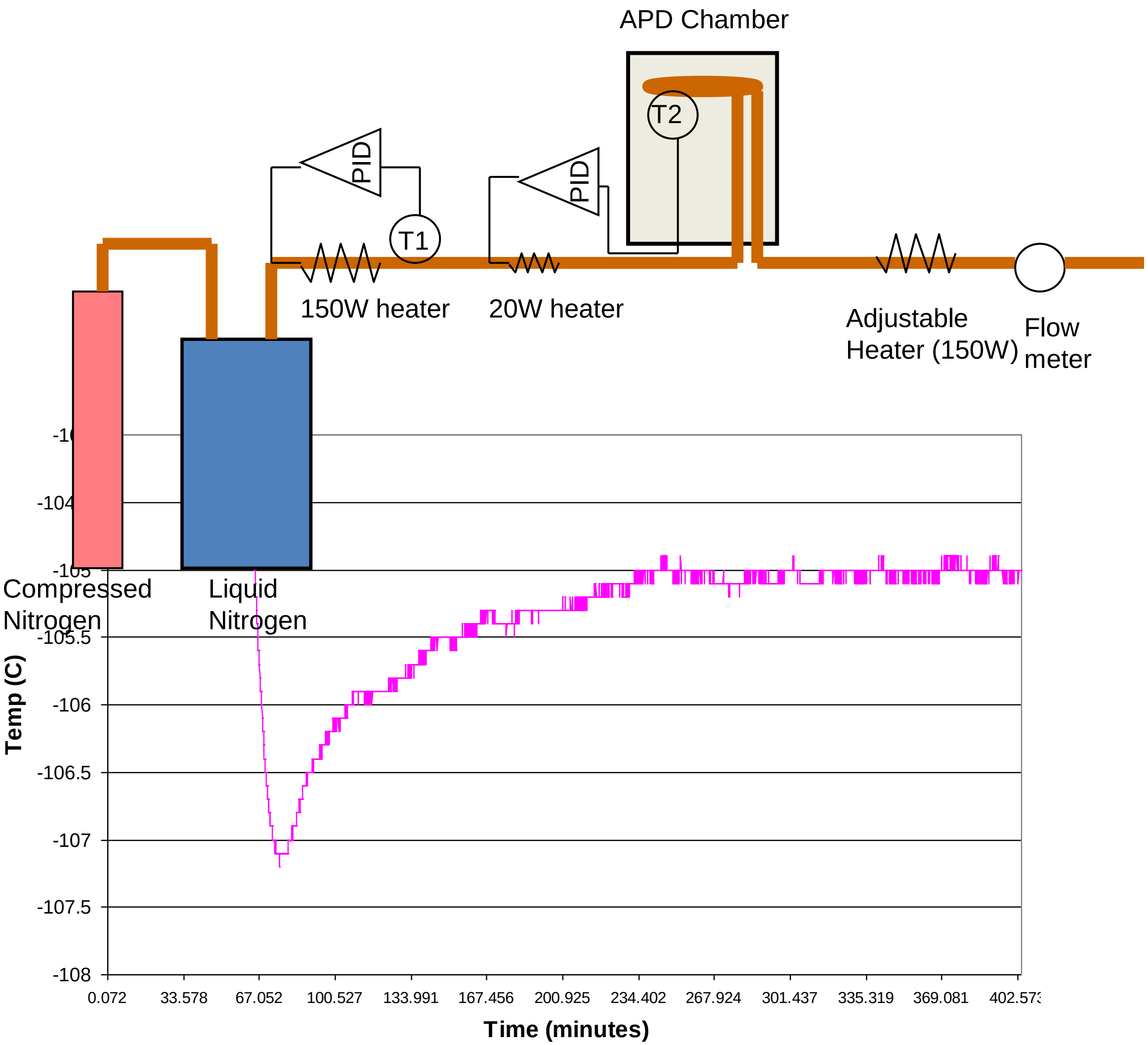

The LAAPDs are cooled at 169K, stable to 0.1K, with two PID loops.

Signal read-out

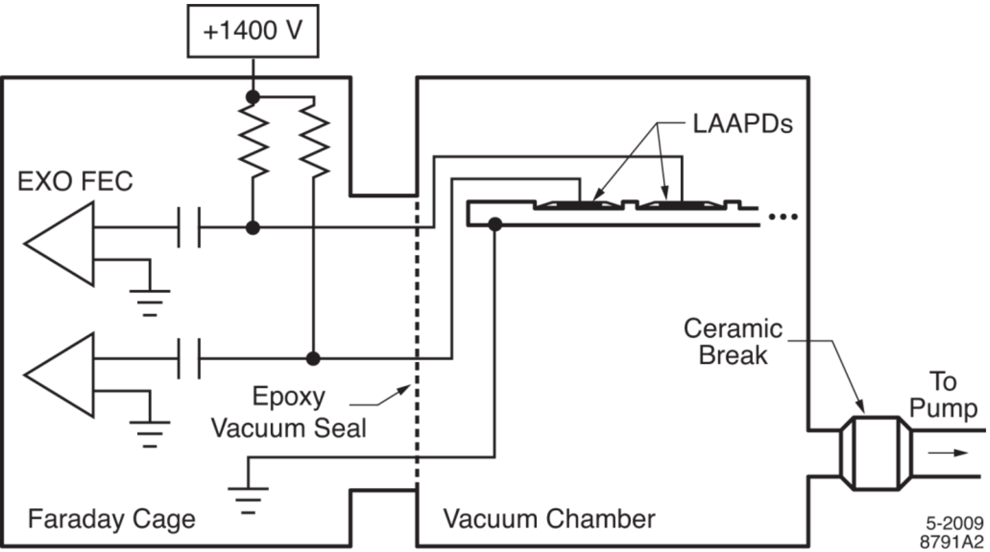

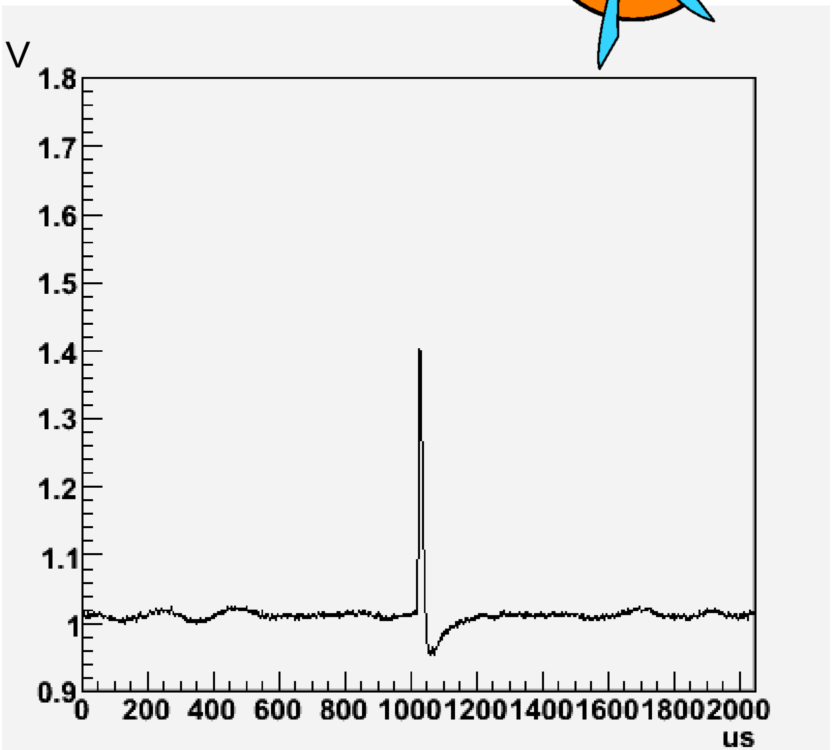

Signal from ^{55}Fe 5.9 keV x-ray.

16 channel EXO-200 Front End Card

LAAPD selection cuts

Relative quantum efficiency

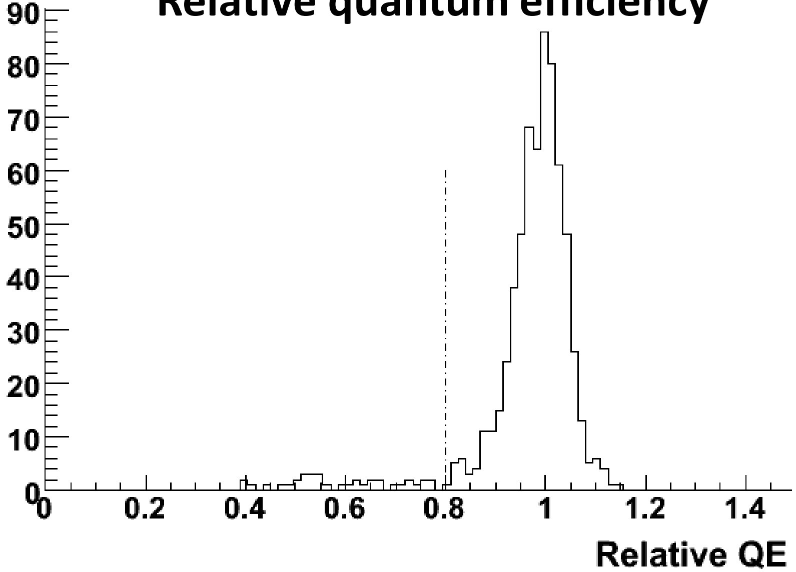

Electronic noise

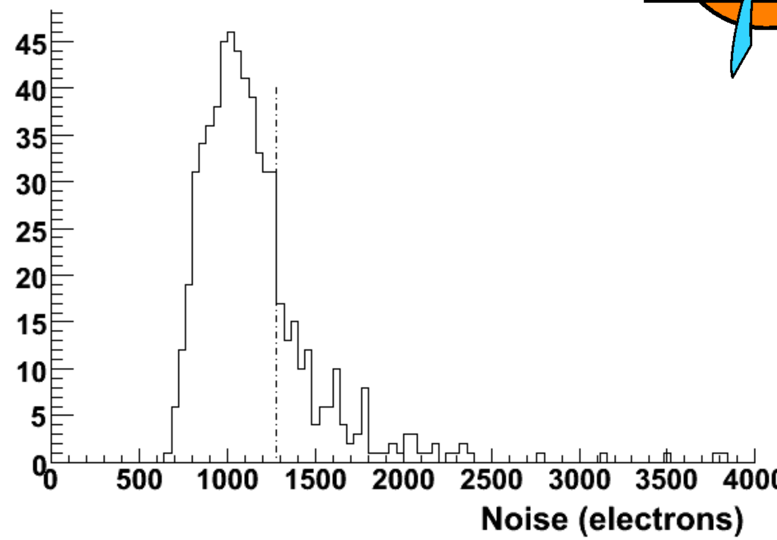

Operating voltage for gain = 100

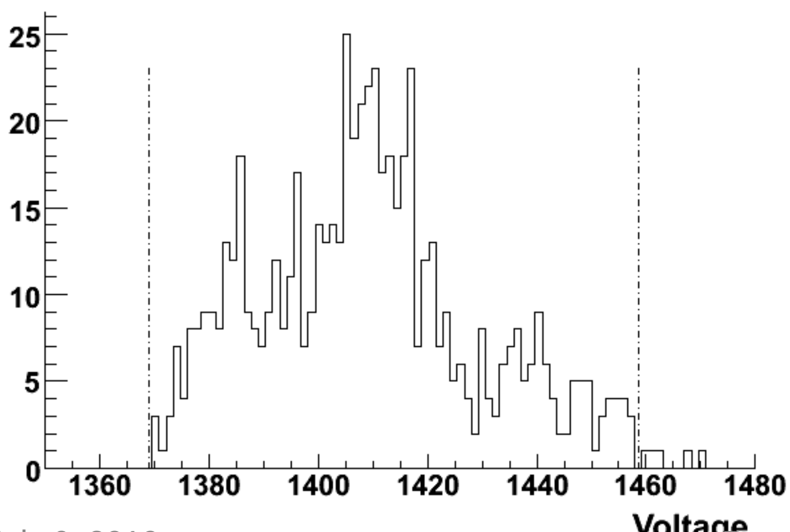

About 180 APDs had noise >> 4000 electrons and were immediately rejected.

R. Neilson et al., NIM A, 608, 68-75

Gain stability

Three APDs were measured in the test chamber over many testing cycles. The properties of these were tested many times to check for variation over time.

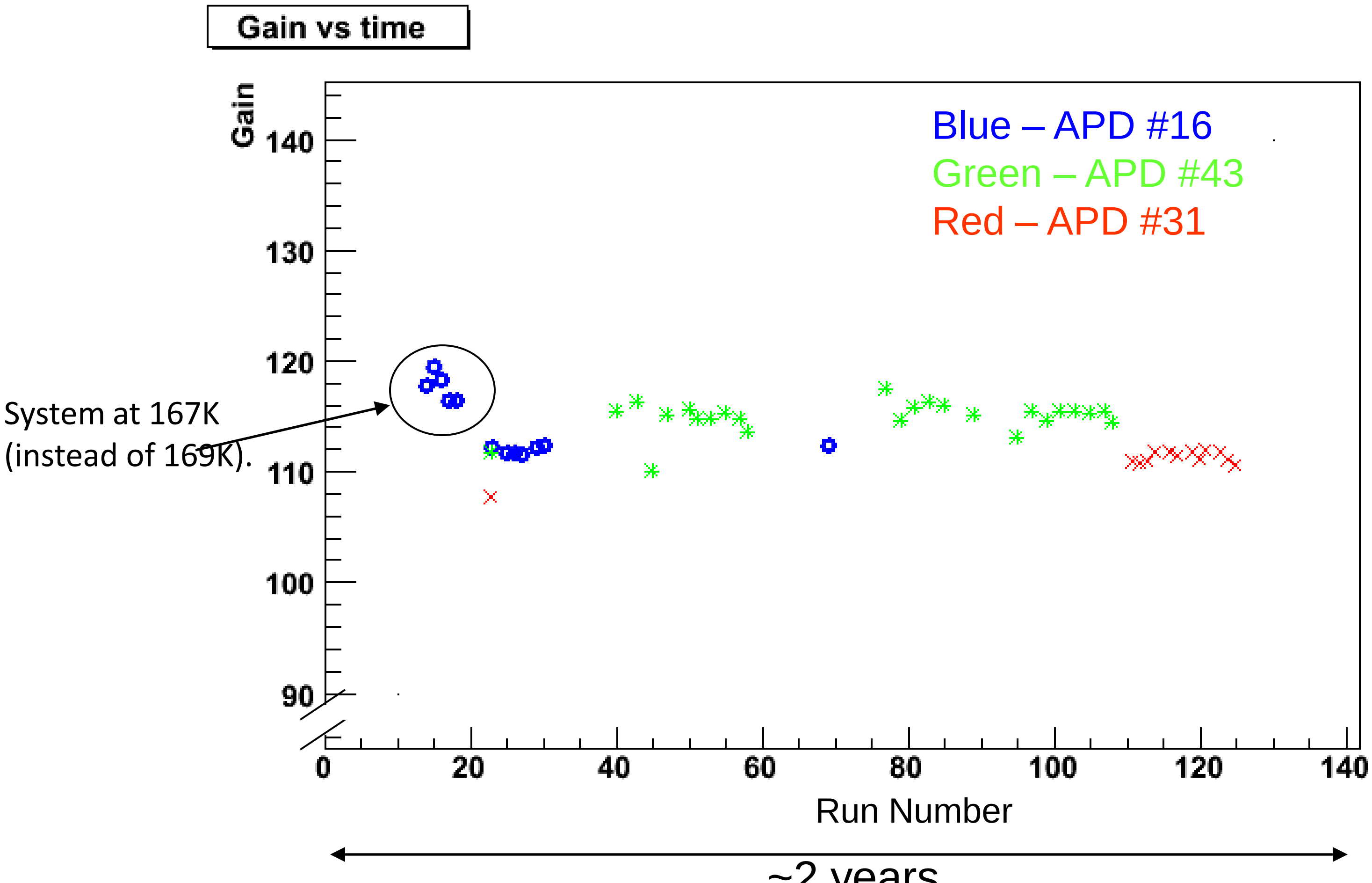

Photon collection efficiency

Simulations (with conservative assumptions) predict photon collection efficiency of ~10-15%

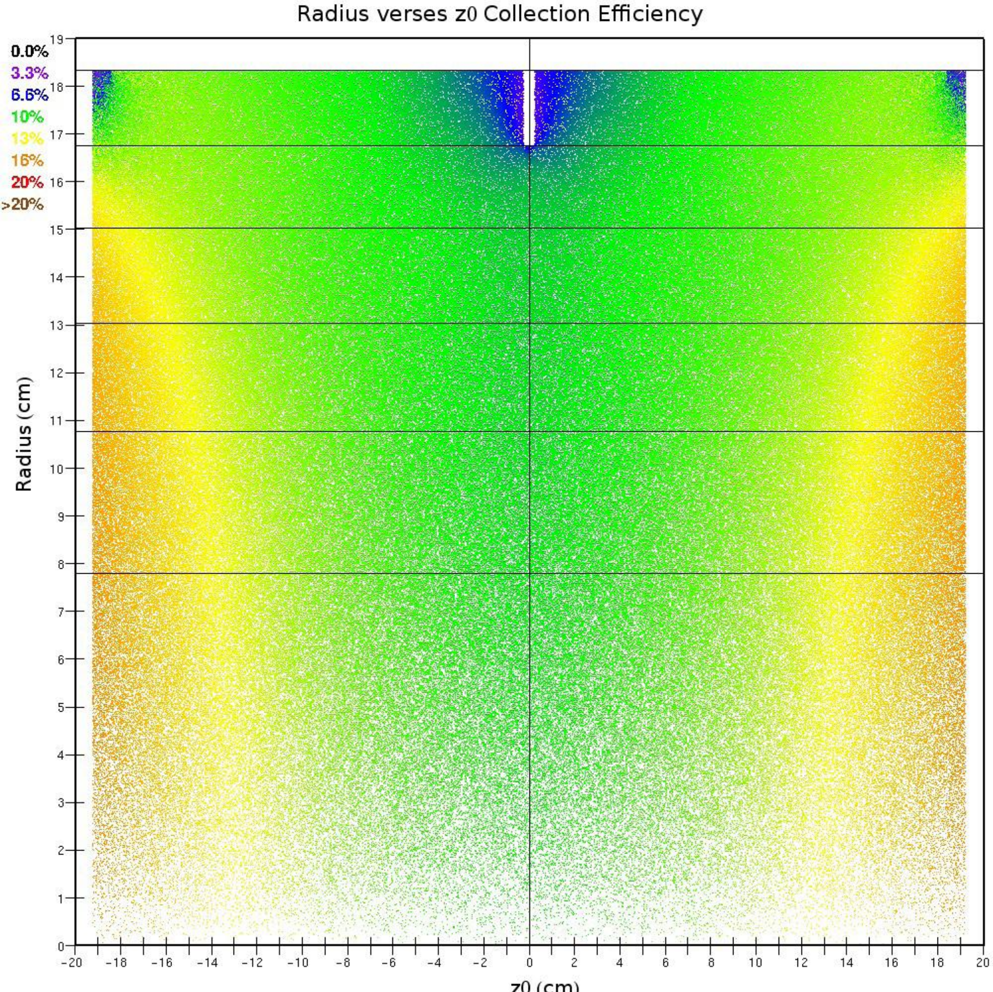

Calibration sources inserted into the cryostat through a copper guide tube

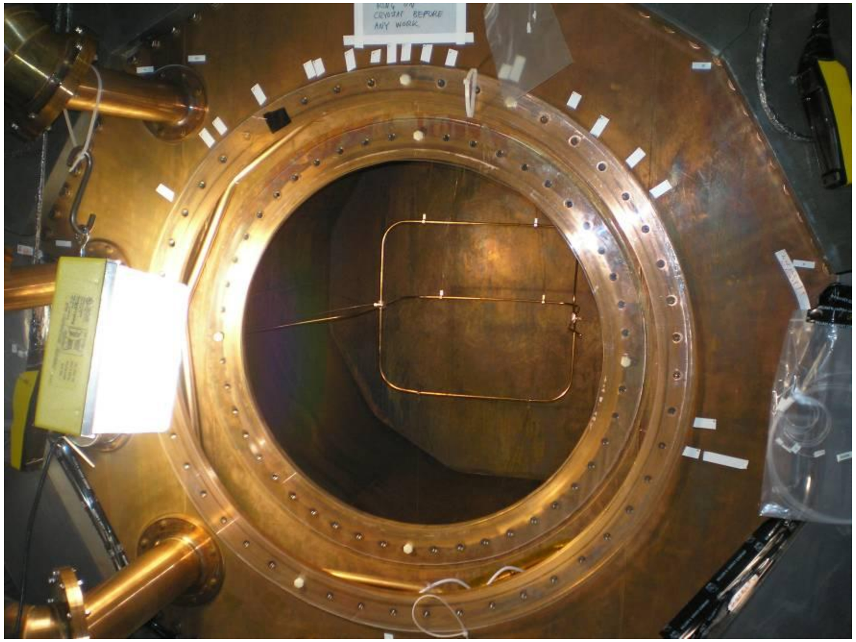

TPC construction

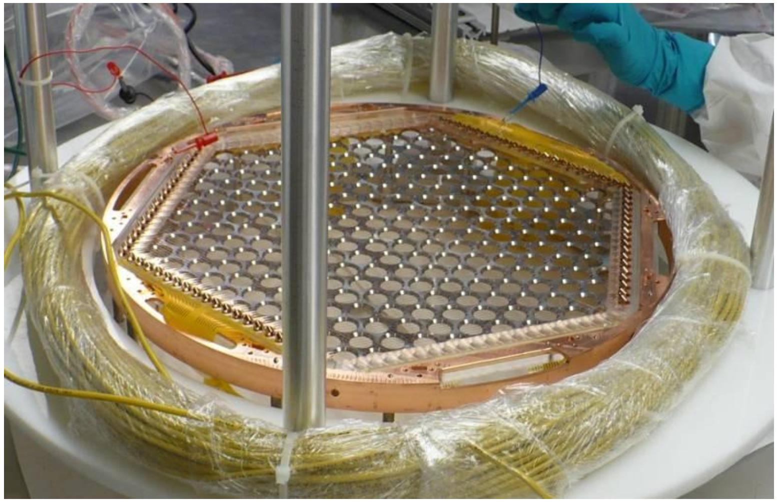

Measuring wire tension

Installing field cages and teflon reflectors

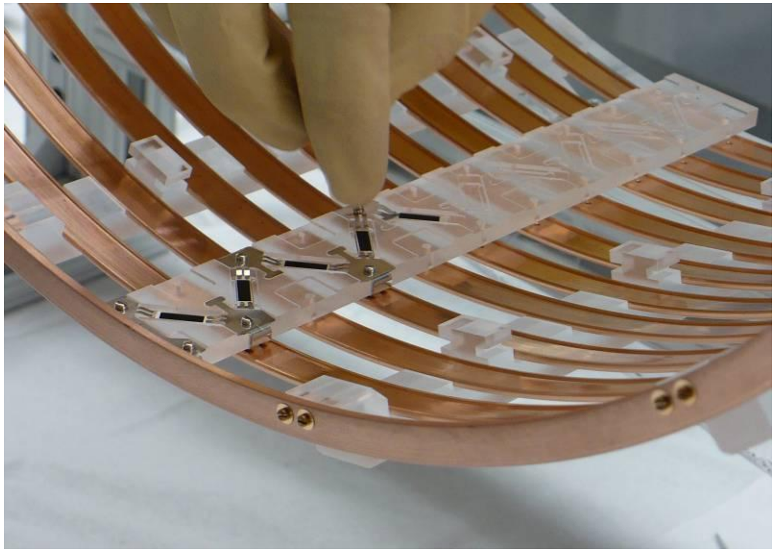

Loading Resistors

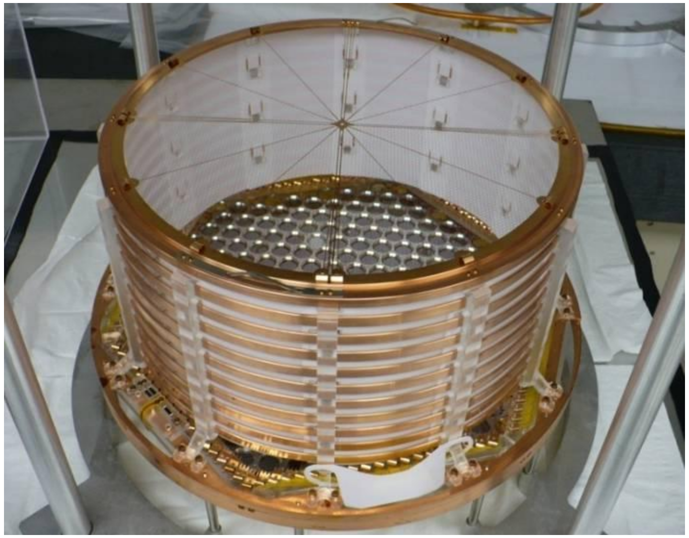

Completed TPC assembly

APD installation

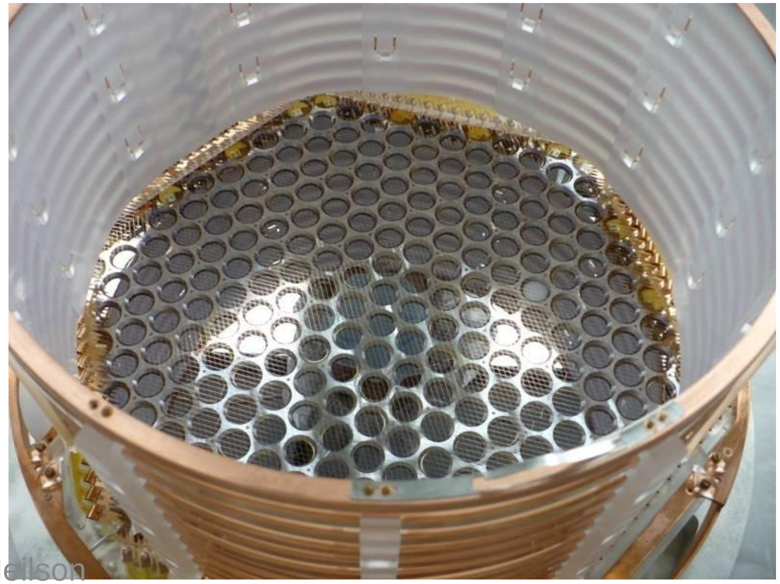

TPC insertion and cabling

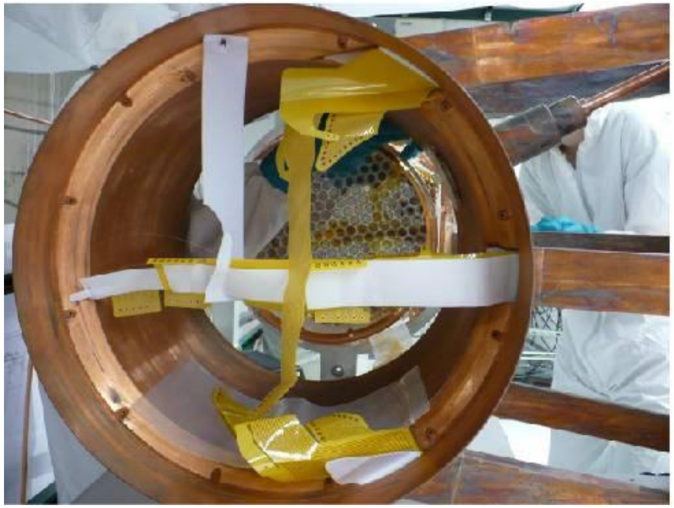

Flex cables inserted in the chamber

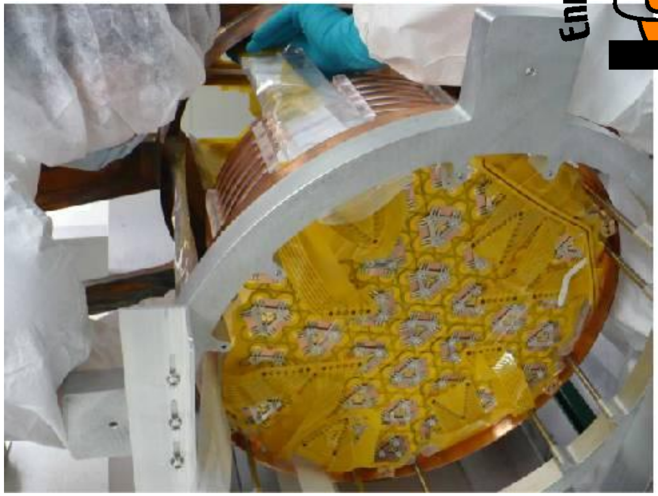

TPC insertion

Detector Wiring

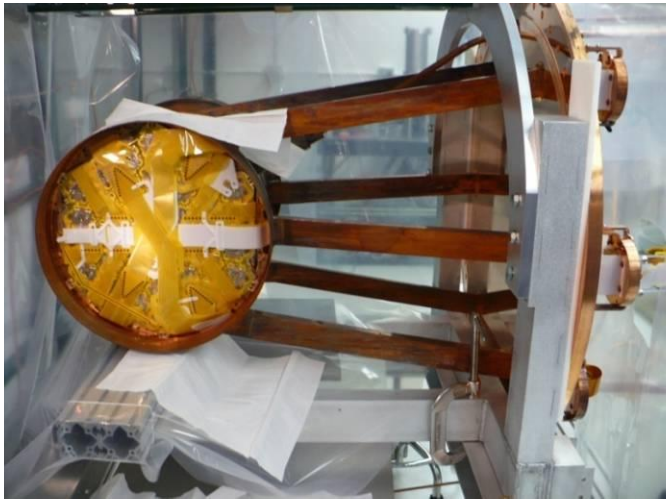

Completed Detector

Laser pulser for in situ LAAPD testing

We inject a pulse from a 406nm laser diode through an optical fiber into a Teflon diffuser in the detector to test APD functionality.

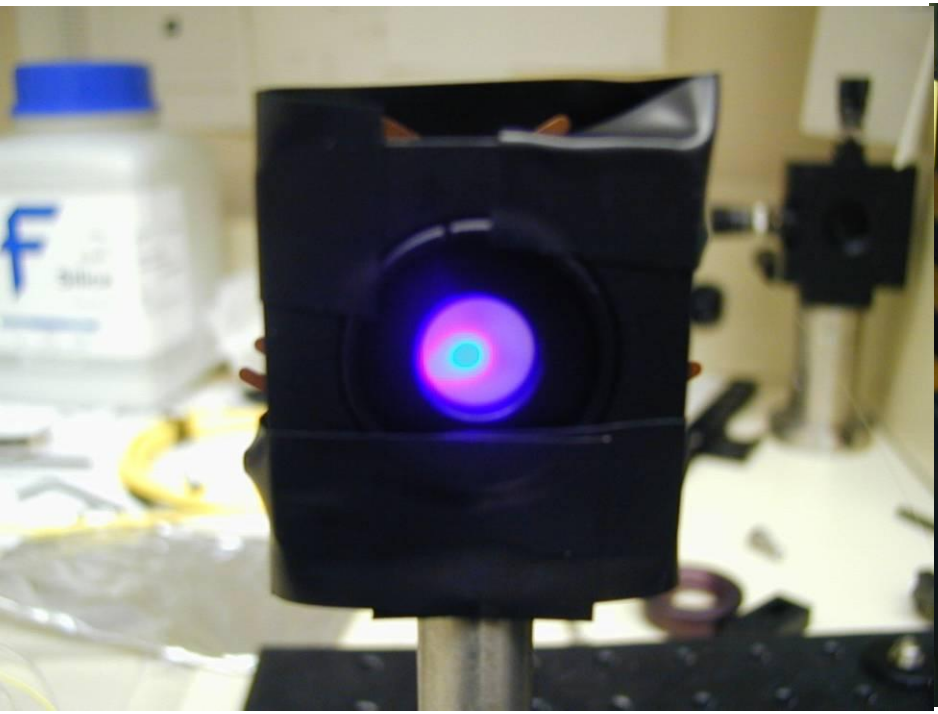

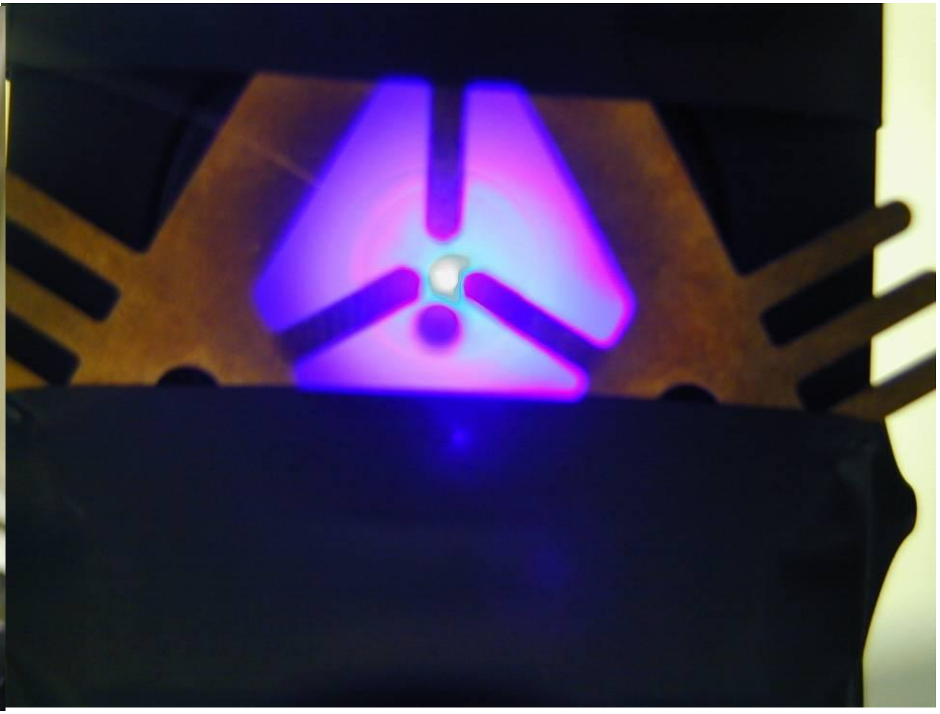

Testing installed LAAPDs at Stanford

The APDs were tested with the laser pulser at Stanford after installation. The tests were done at room temperature in a boil-off nitrogen gas environment and only at very low bias voltage.

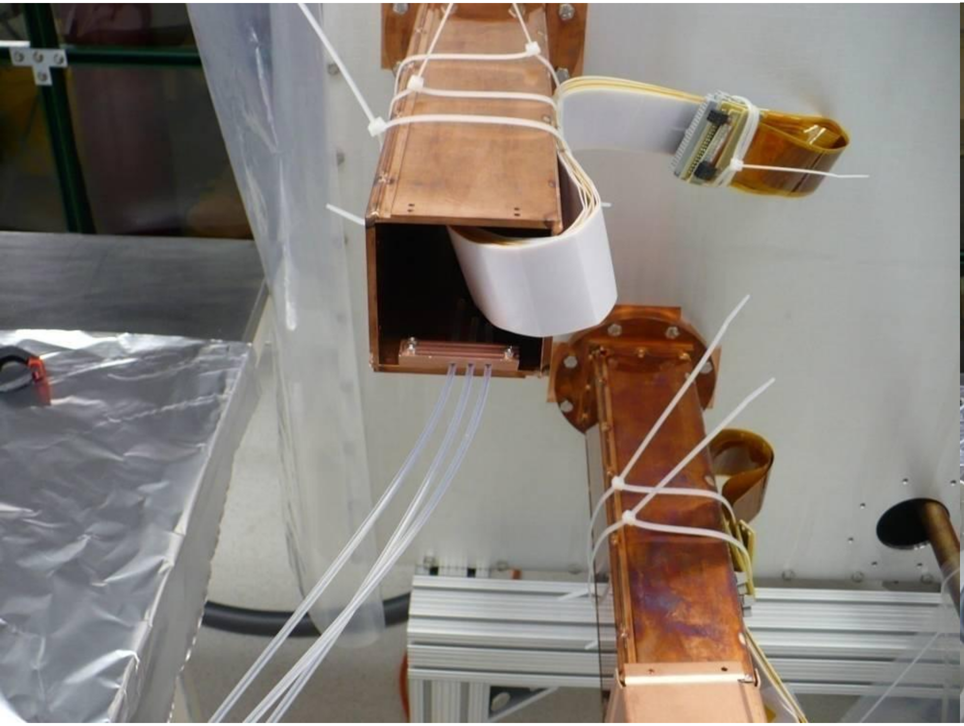

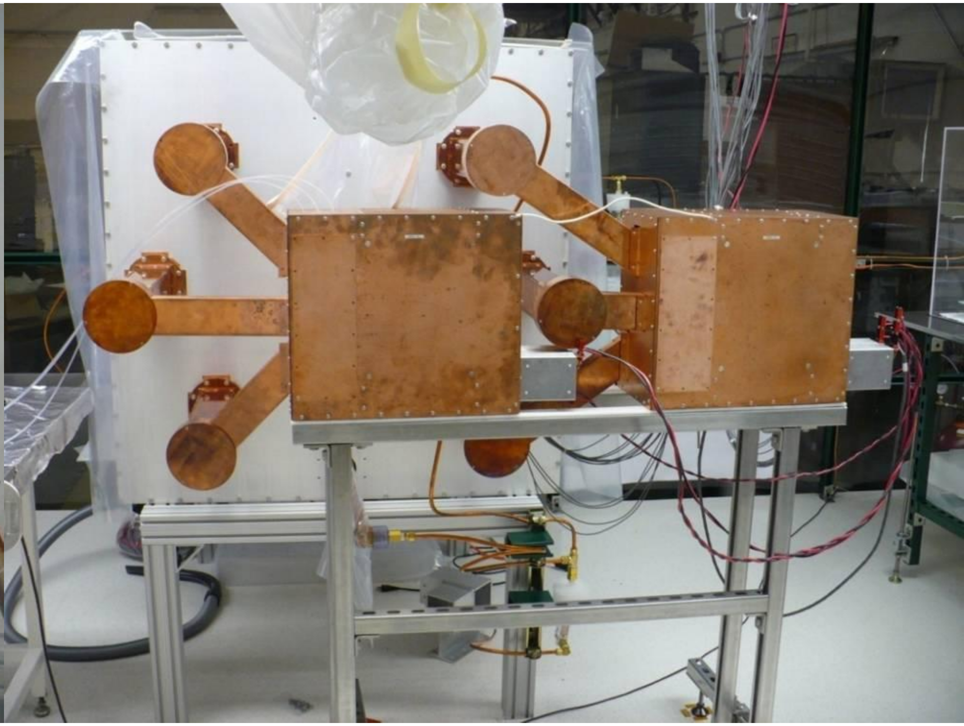

Laser pulser LAAPD signals

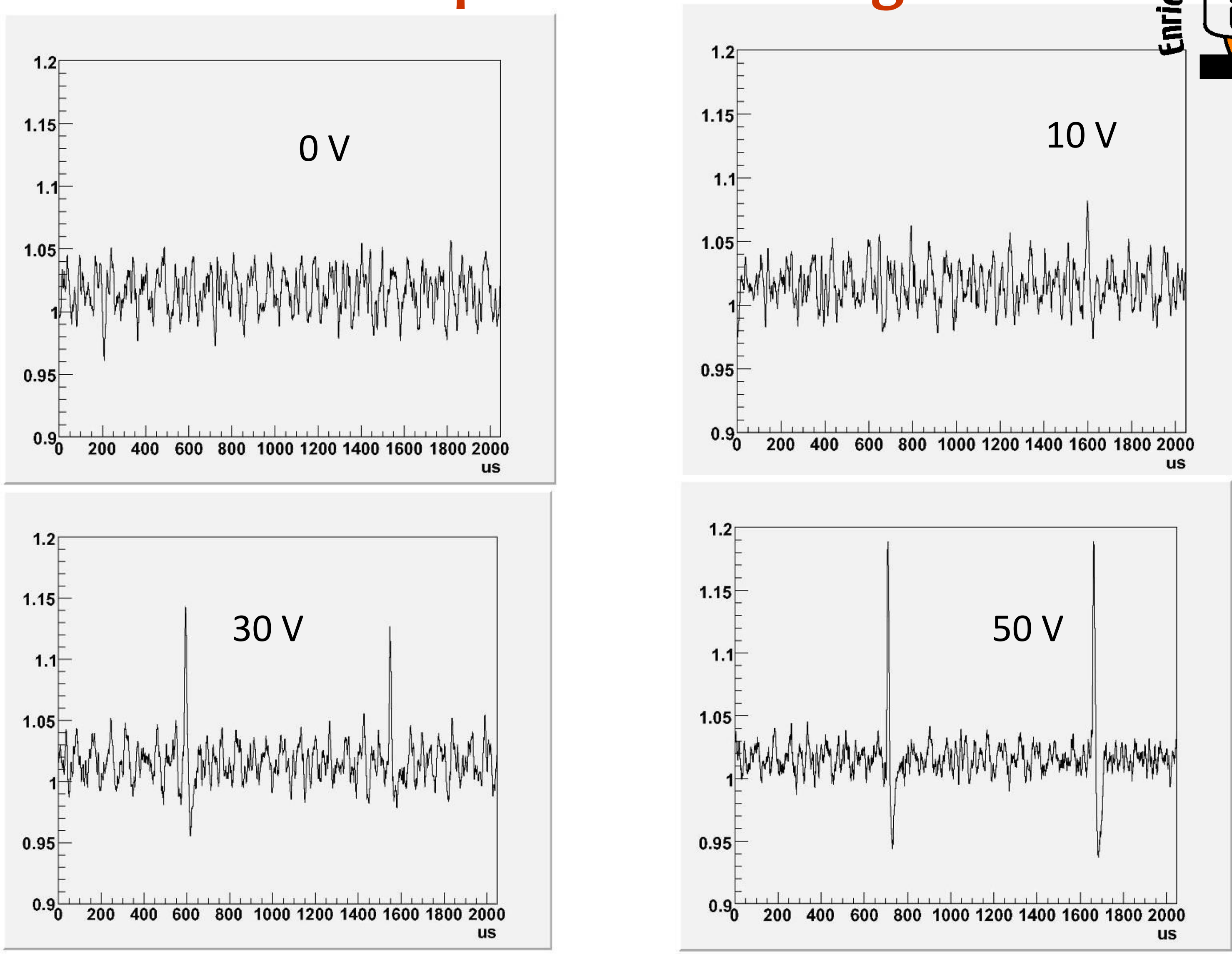

1 kHz laser pulser, TPC filled with nitrogen gas at STP

Laser pulser signals for multiple LAAPD gangs with 50V bias

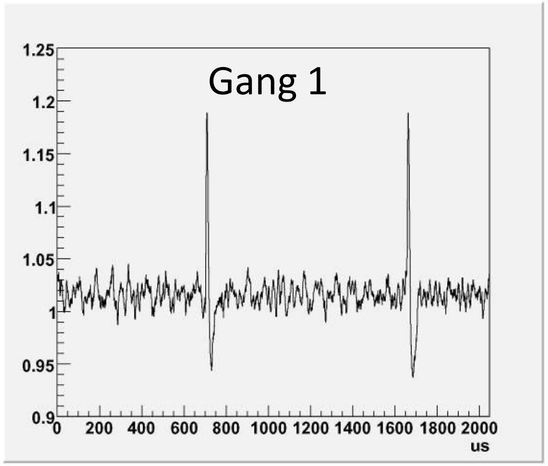

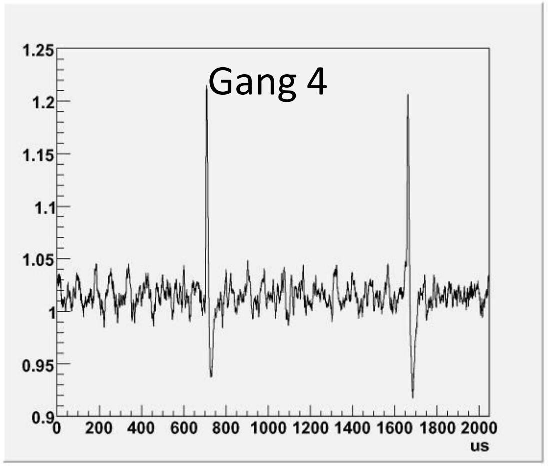

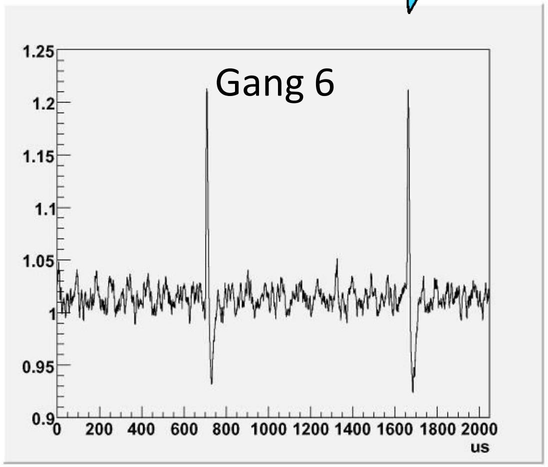

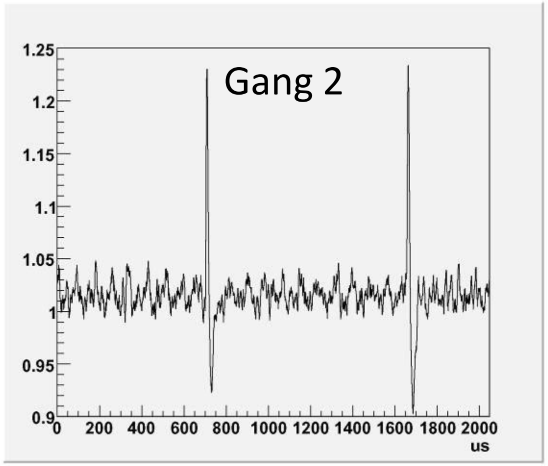

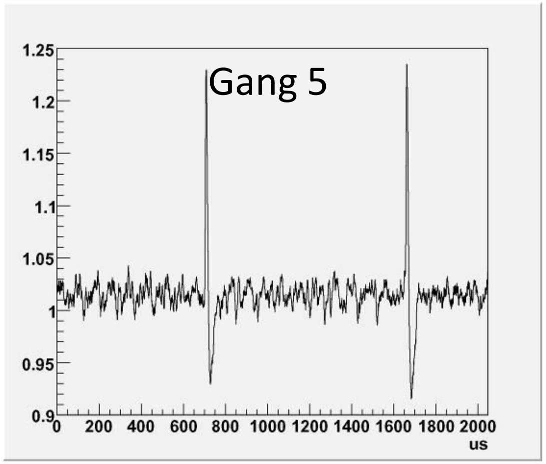

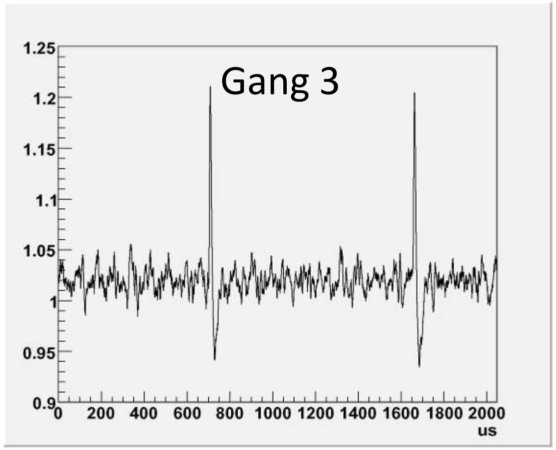

Event display for laser pulser

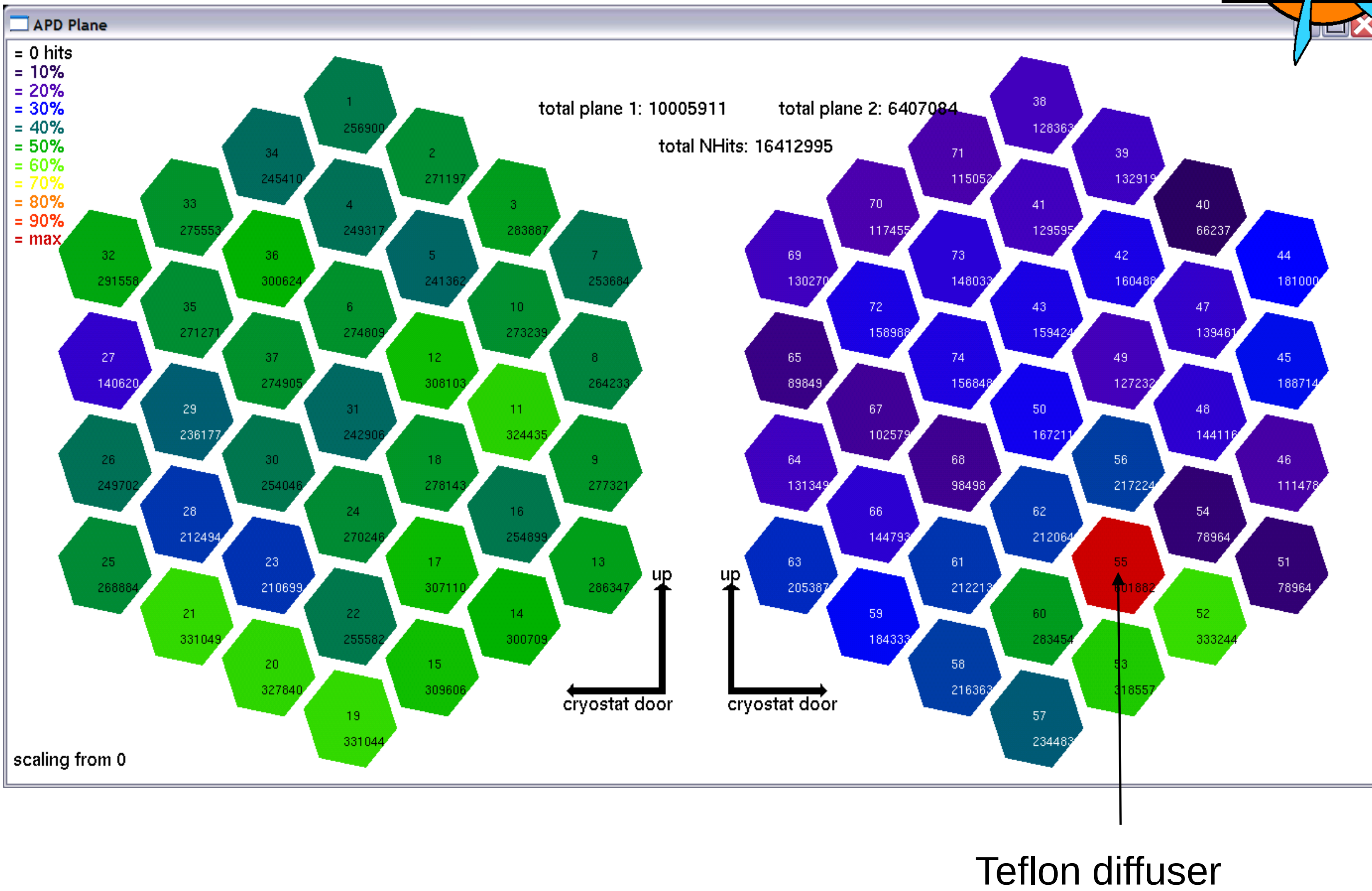

Liquid xenon energy resolution

Microscopic anti-correlation between ionization and scintillation.

Reading out both gives improved energy resolution.

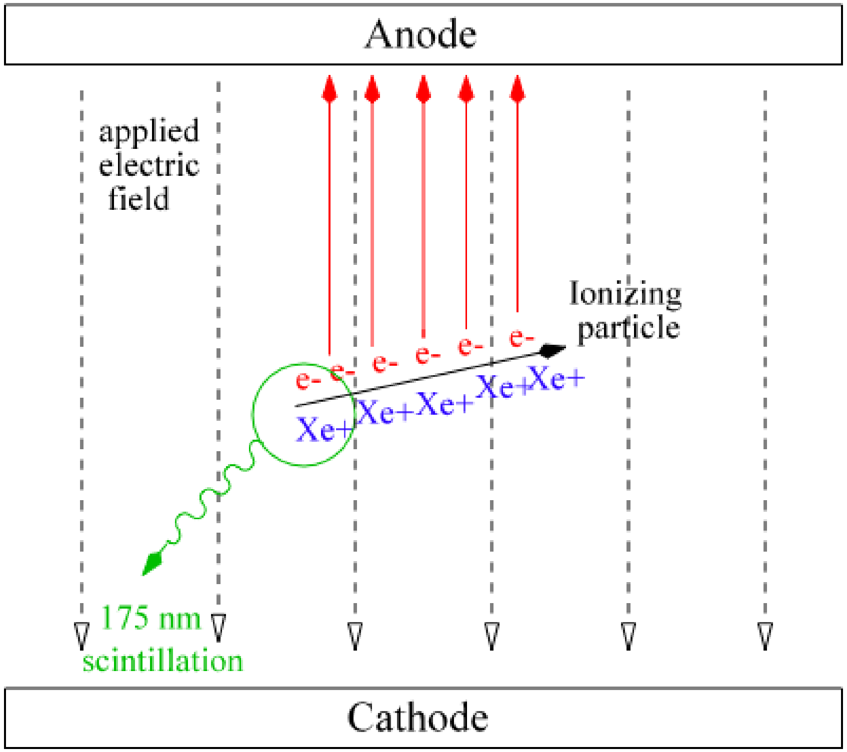

1 kV/cm drift field, ^{207}Bi EC source

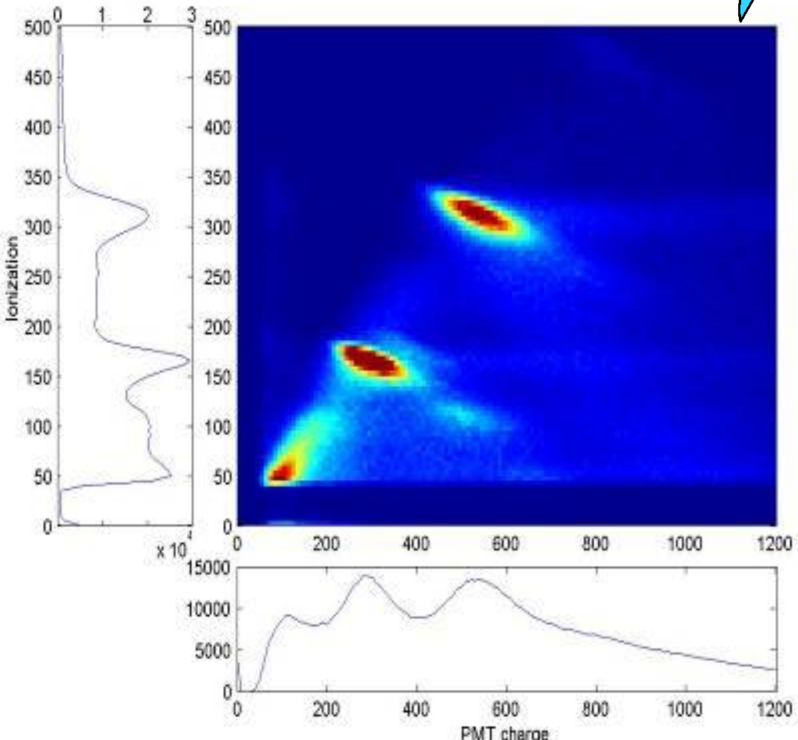

[E. Conti et al., PRB: **68**(2003)054201]

Ionization only:

$\sigma(E)/E$ = 3.8% at 570keV gives 1.8% at $Q_{\beta\beta}$

Ionization and Scintillation:

$\sigma(E)/E$ = 3.0% at 570keV gives 1.4% at $Q_{\beta\beta}$

Recombination model

Data from 1.5L Stanford LXe chamber

Geant4 simulation with a deterministic recombination model based on C.E. Dahl's thesis (Princeton University, 2009)

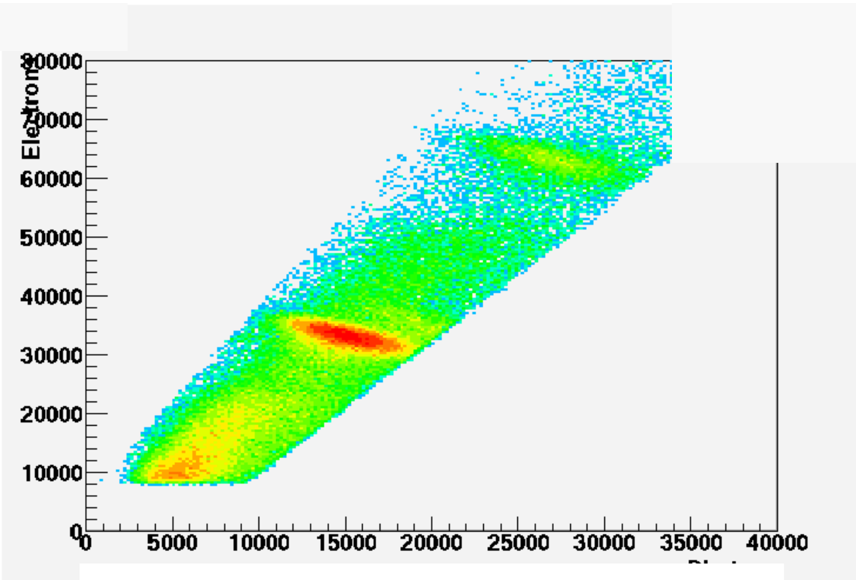

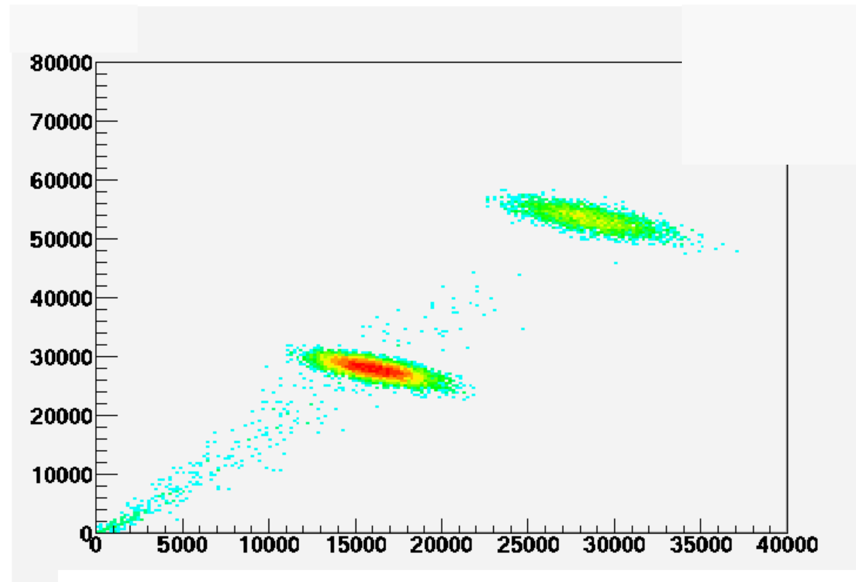

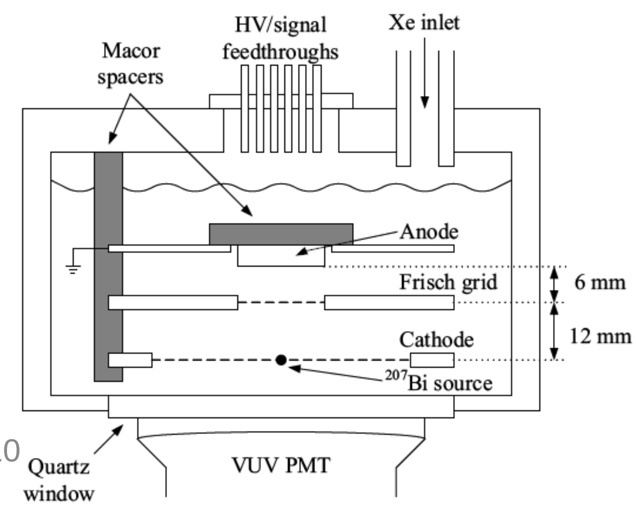

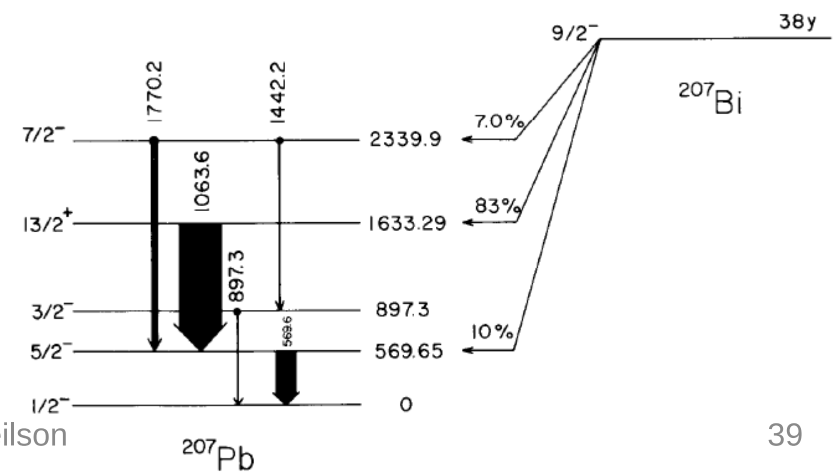

EXO-200 Electronics

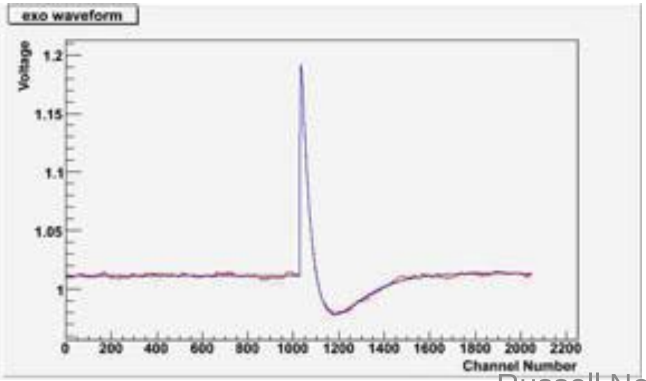

EXO-200 signal read-out

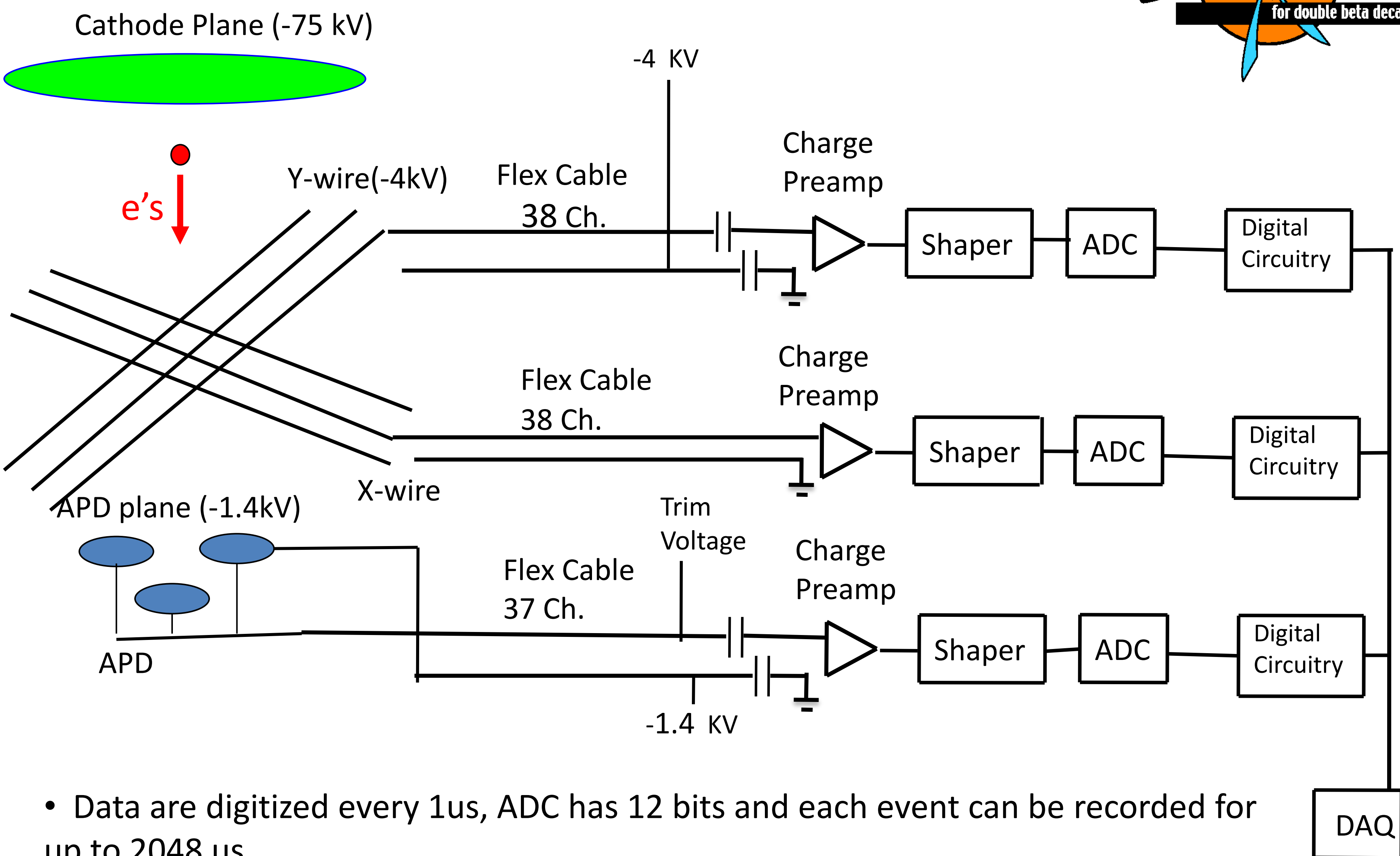

- Data are digitized every 1us, ADC has 12 bits and each event can be recorded for up to 2048 us.

Event reconstruction

Simulated 0νββ event with bremsstrahlung photon.

X-wire (collection wire) signals

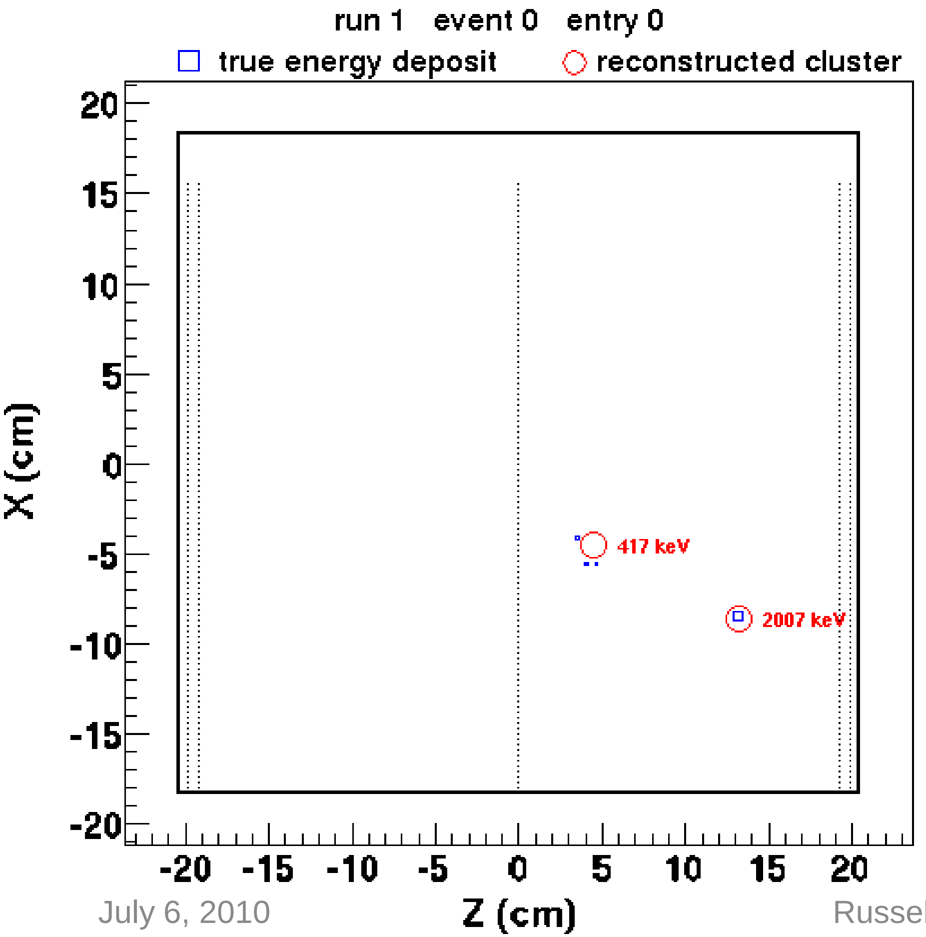

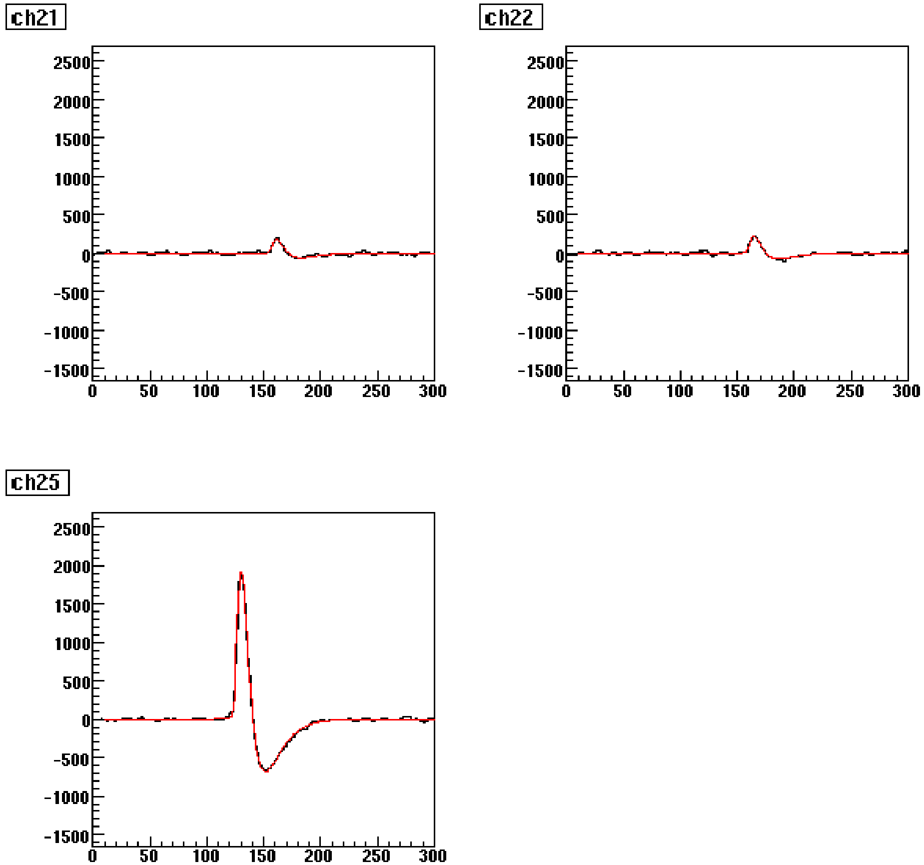

Reconstruction with light only

Error in reconstructed position

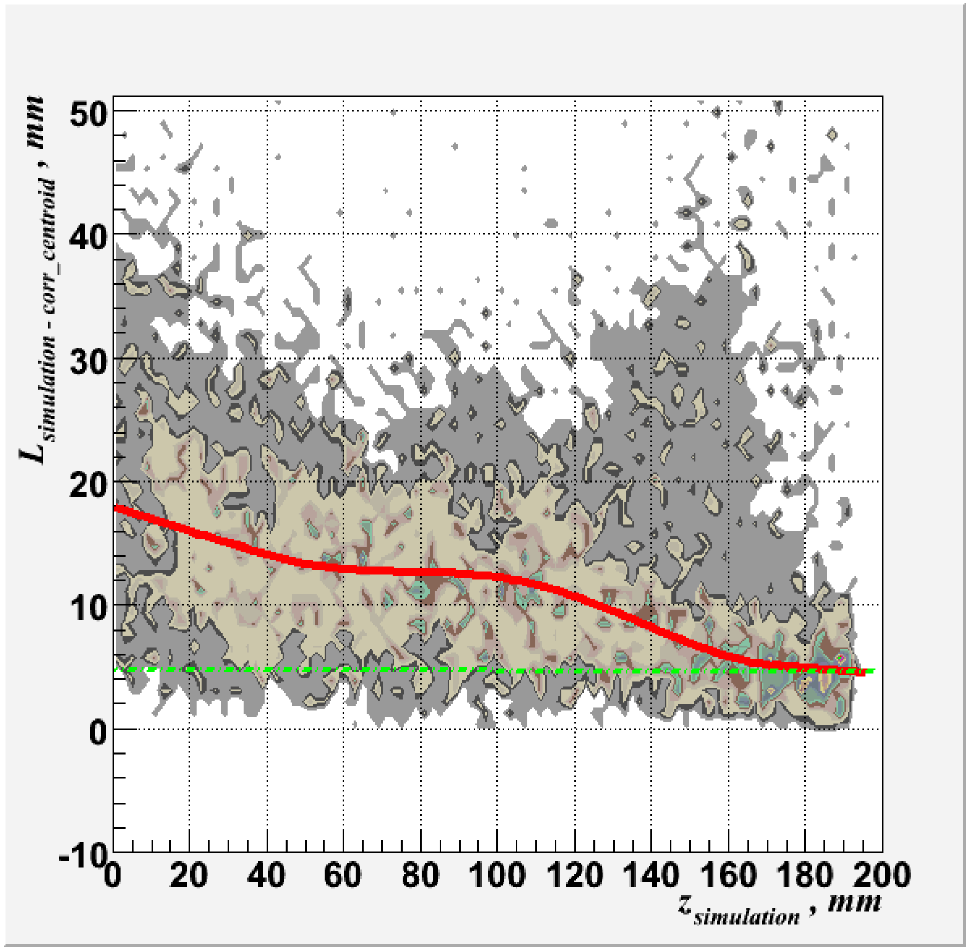

It is also possible to do position reconstruction with LAAPD signals only to complement the x-y wire reconstruction.

Magnetic xenon pump

Enriched Xenon Observatory for double beta decay

Outer ring magnet

Highly polished SS tube

SS flappers on 4-5/8 conflats

Linear motion system

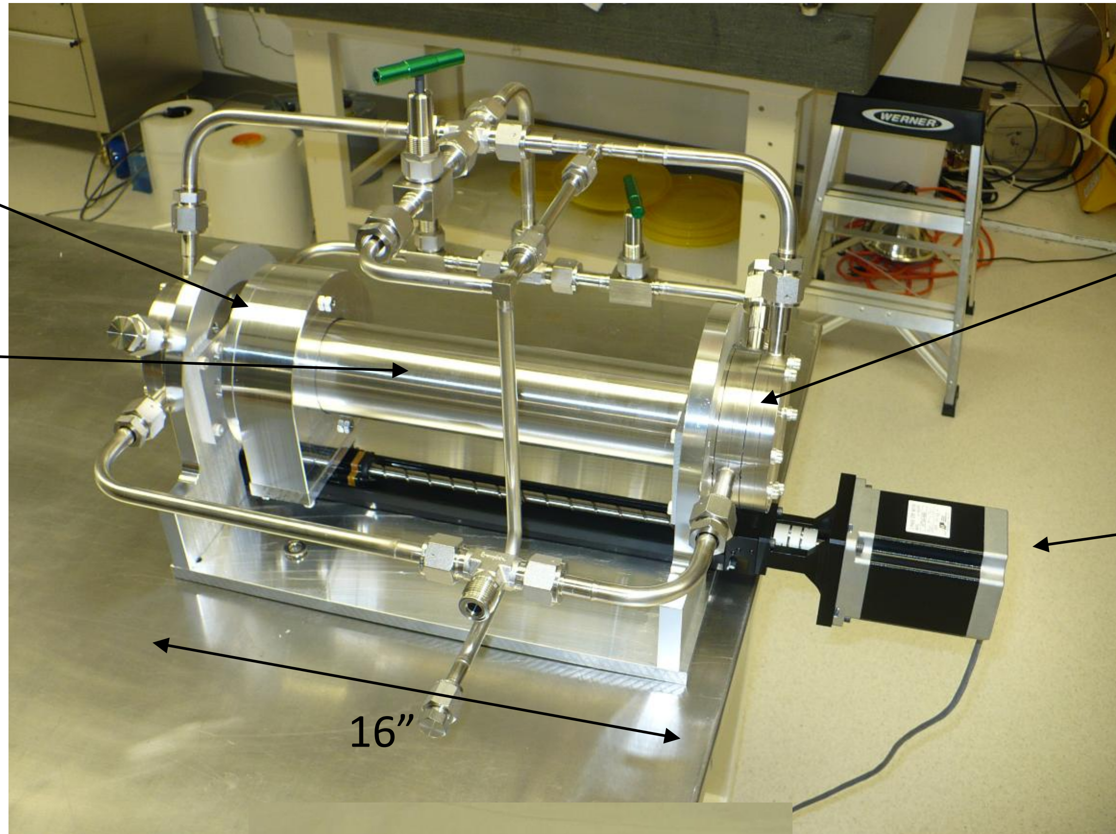

Inner magnet welded in SS can

UHMW polyethylene gaskets

3.5”

Xenon recirculation

Uses for pump :

- Recirculate xenon while the TPC is full of liquid.
- Recirculate room temperature gas xenon to remove impurities.
- Increase condensation rate during LXe filling stage.

Magnetic coupling

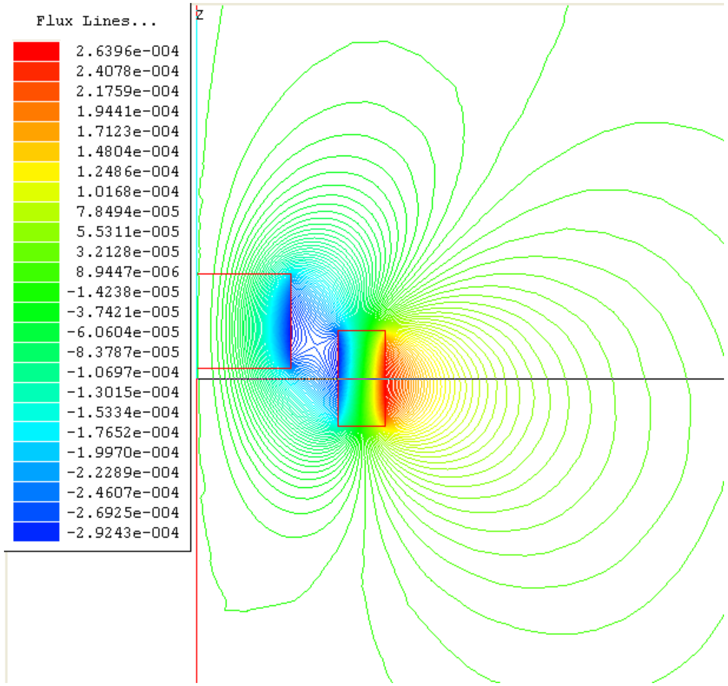

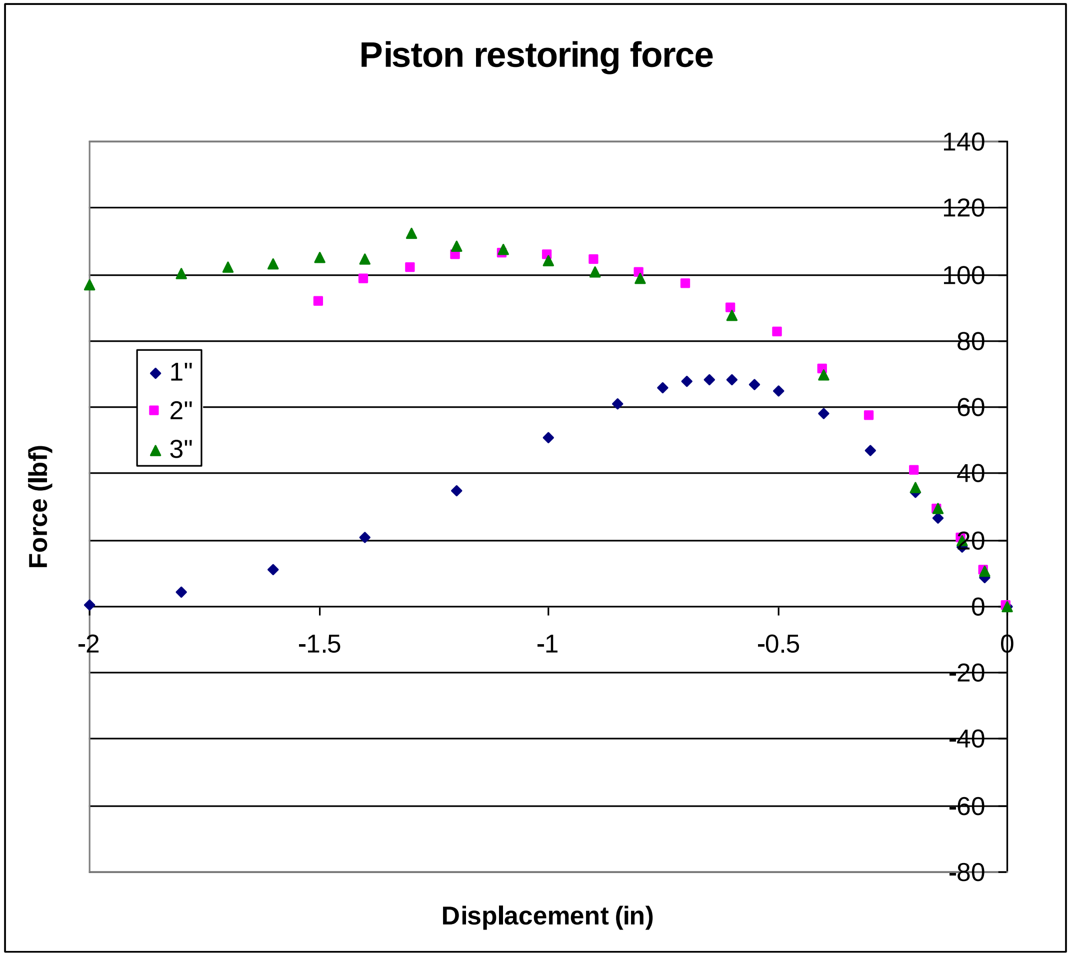

Calculated maximum pumping pressure without decoupling

- 1” magnets – 13.9 psi
- 2” magnets – 21.6 psi
- 3” magnets – 22.5 psi

Circulating xenon gas

Xe Flow (SLPM)

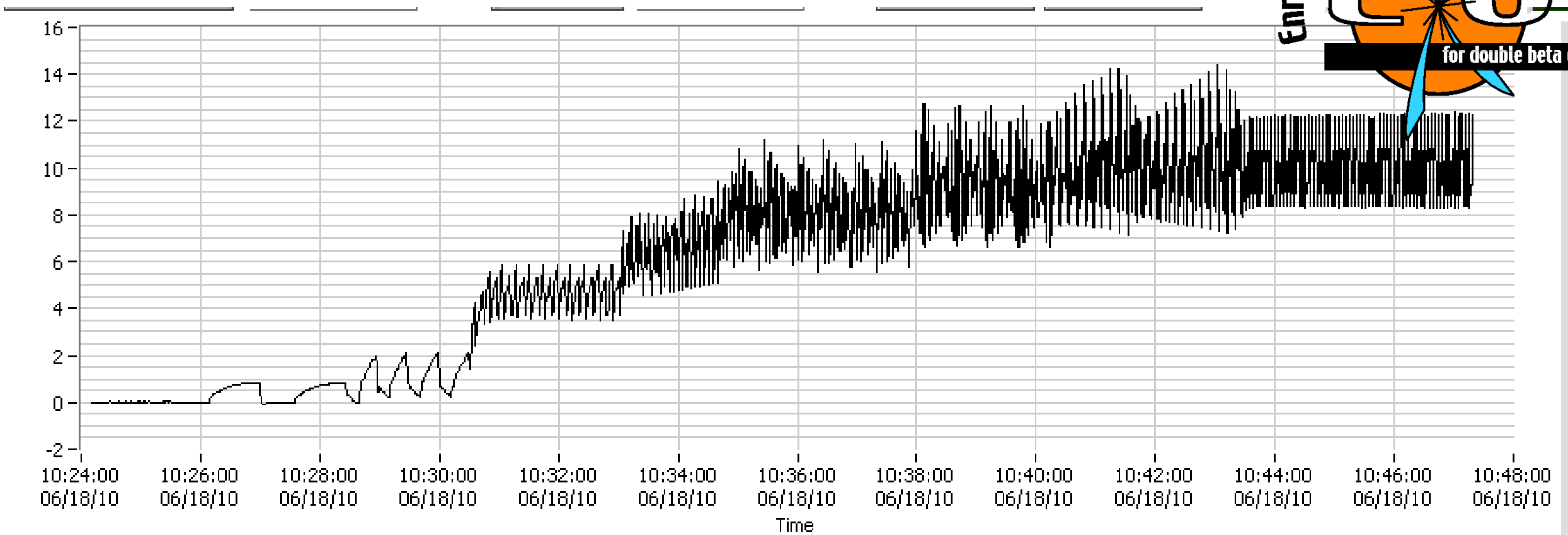

Pressure (torr)

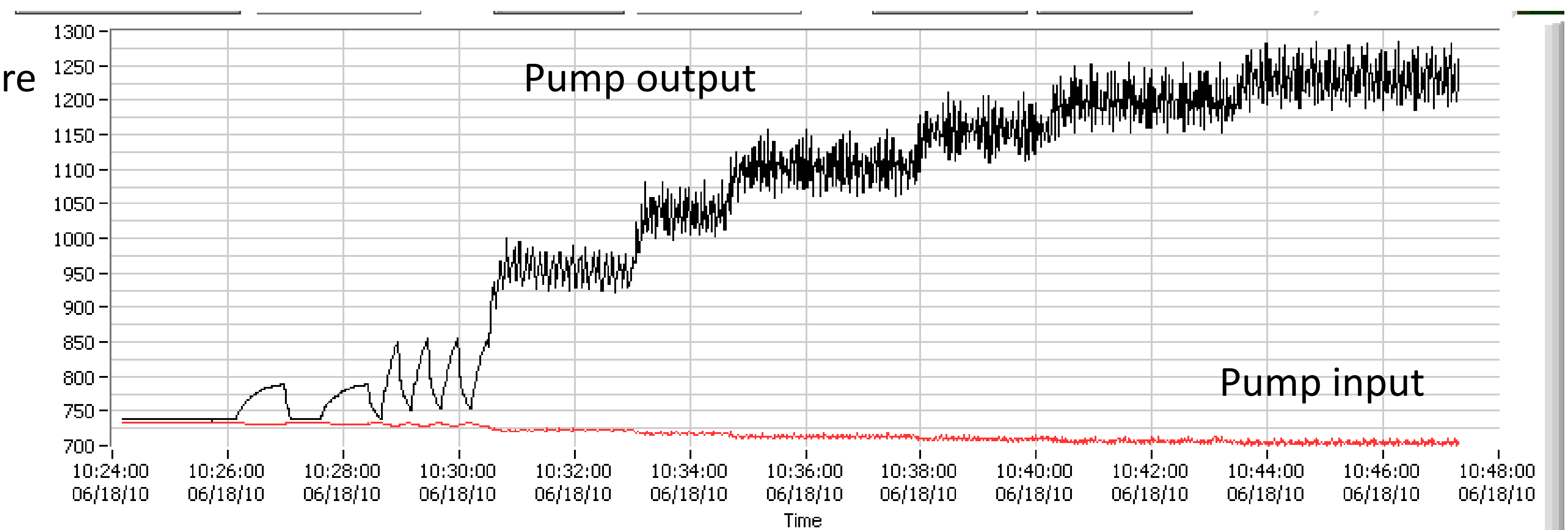

Enriched Xenon Observatory
for double beta decay

Active muon veto

•Active muon veto system installed 2009

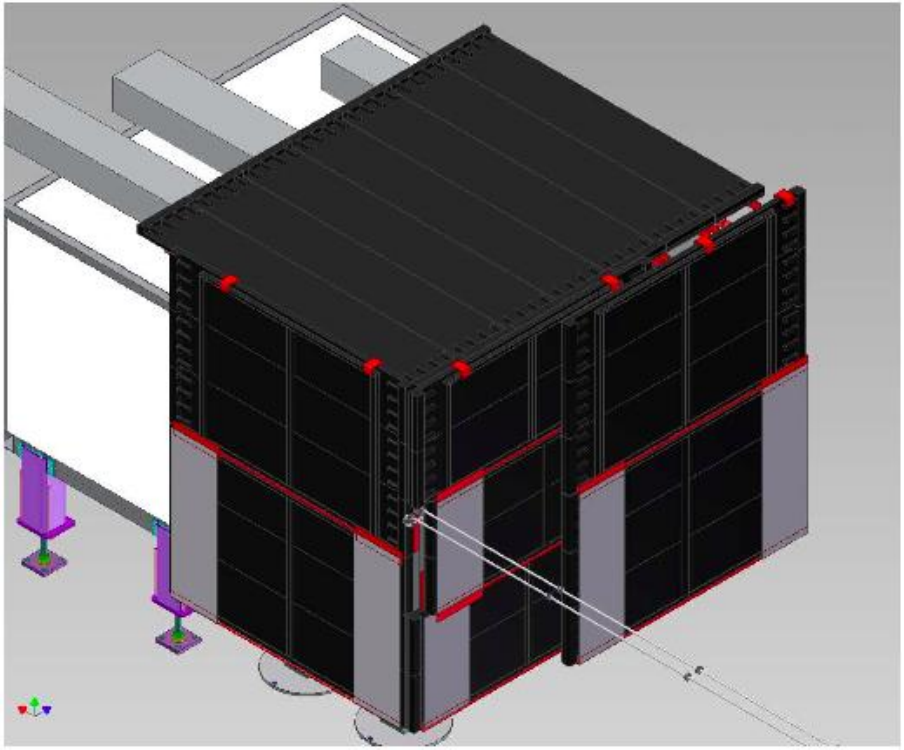

TPC installation

Jan 2010

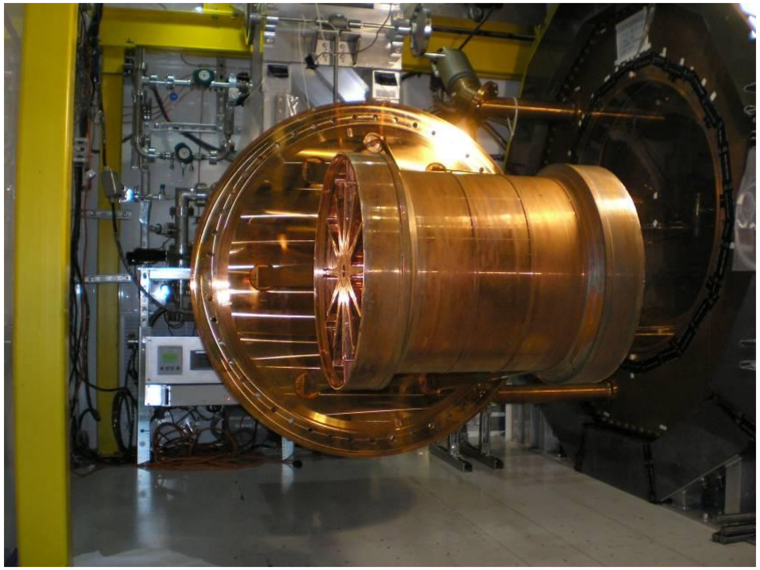

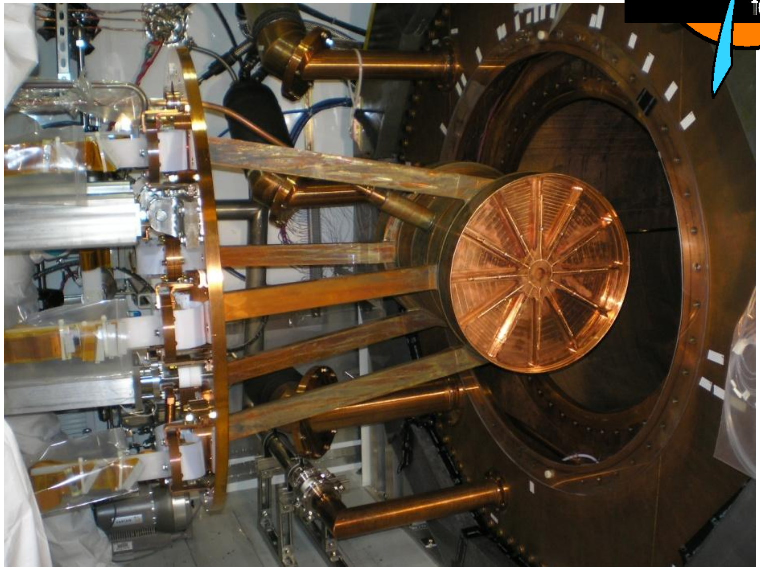

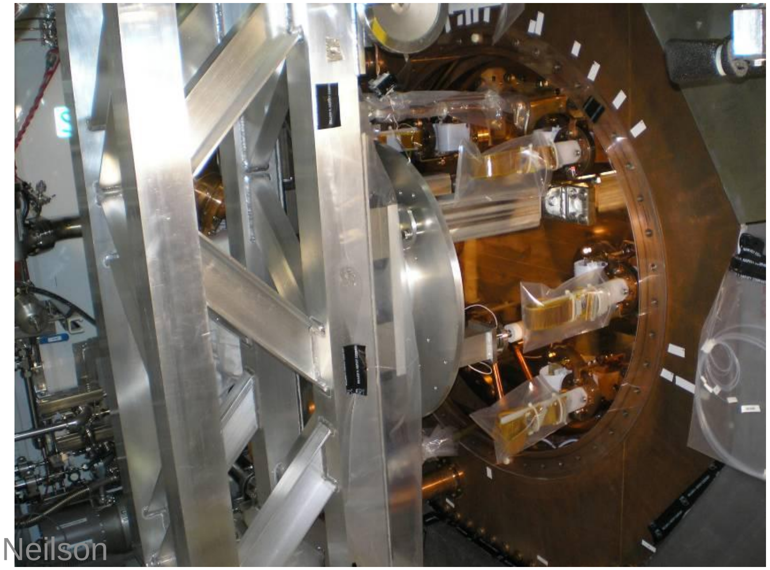

Installed electronics

Feb 2010

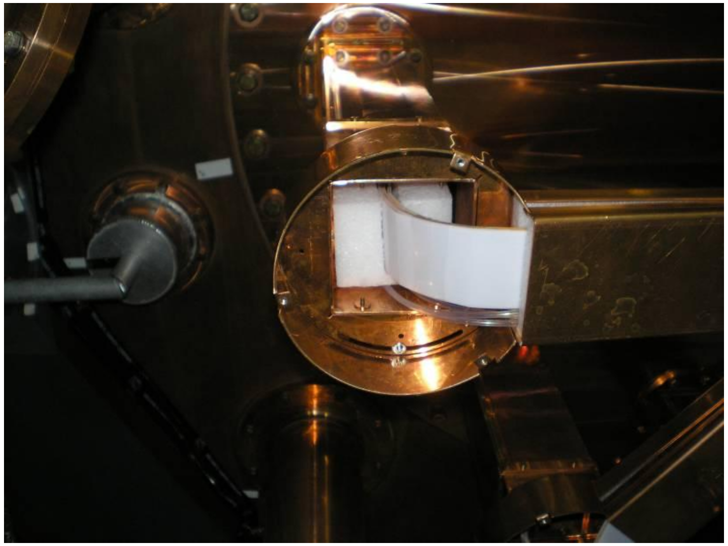

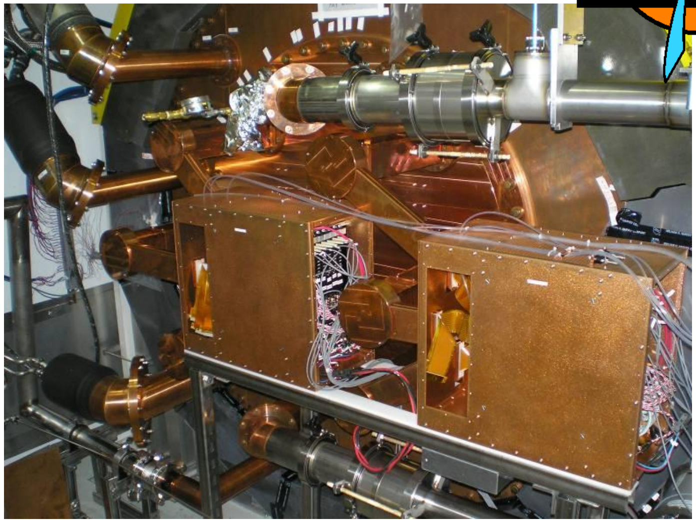

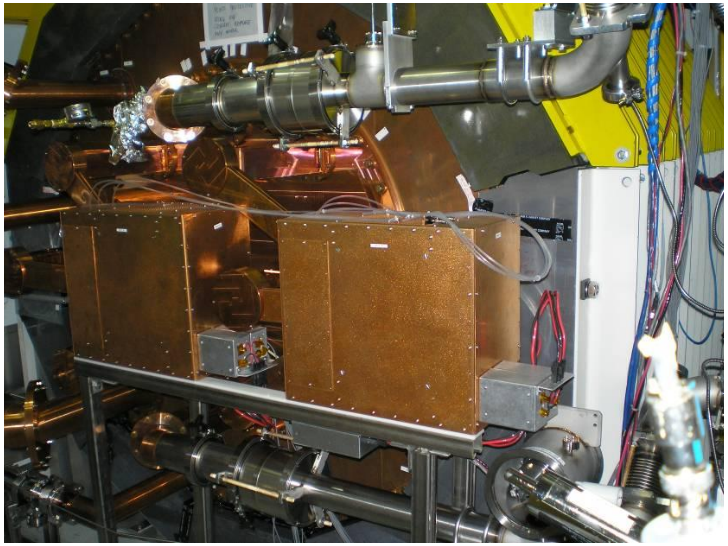

Noise at expected levels

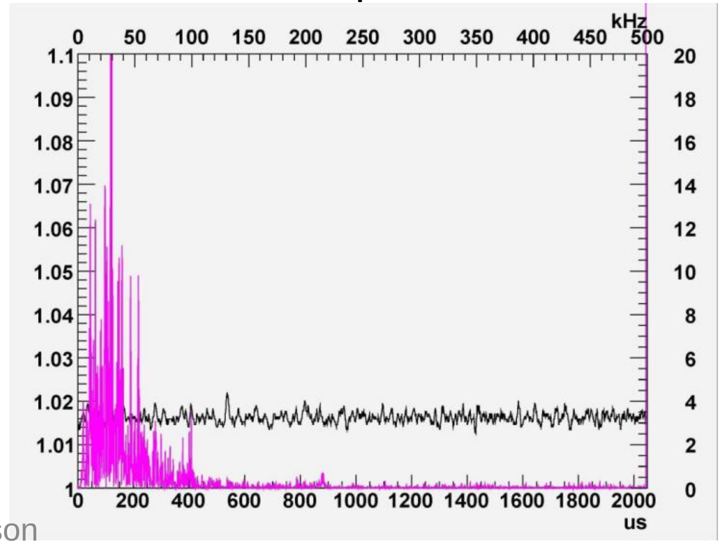

Gas recirculation and purity measurements

Since May 2010

We are currently circulating room temperature natural xenon gas.

Gas purity monitor

Electronegative impurities detected by measuring their effect on emission from a tungsten filament

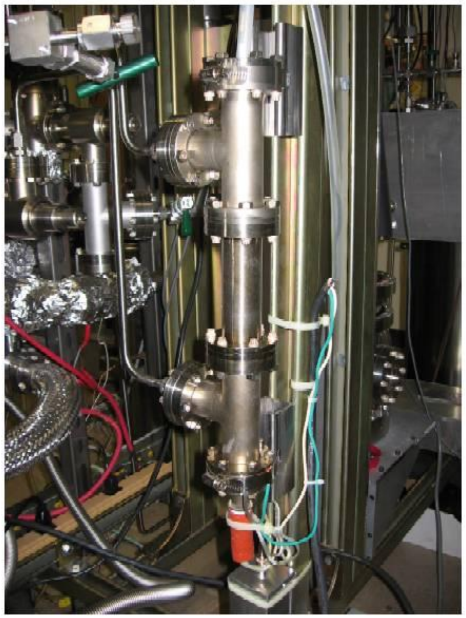

Xenon cold trap

Xenon is frozen out to allow measurements of impurities below 1ppb with an RGA.

Xenon purity is looks continuously improving.

EXO-200: sensitivity

2 year sensitivities for the EXO-200 $0\nu\beta\beta$ search.

Case	Mass (ton)	Eff. (%)	Run Time (yr)	σ_E/E @ 2.5MeV (%)	Radioactive Background (events)	$T_{1/2}^{0\nu}$ (yr, 90%CL)	Majorana mass (meV)	
							QRPA[1]	NSM[2]
EXO-200	0.2	70	2	1.6*	40	$6.4*10^{25}$	109	135

1. Simkovic et al., *Phys. Rev.* C**79**, 055501(2009) [g_A= 1.25]; 2. Menendez et al., *Nucl. Phys.* A**818**, 139(2009) [UCOM results]

EXO-200 will also search for $2\nu\beta\beta$ of ^{136}Xe, which has not been observed.

	$T_{1/2}^{2\nu}$ (yr)	Events/year (no efficiency applied)
Experimental limit		
Luescher et al, 1998	**> 3.6×10^{20}**	**< 1.3 M**
Bernabei et al, 2002	**> 1.0×10^{22}**	**< 48 k**
Gavriljuk et al, 2005	**> 8.5×10^{21}**	**< 56 k**
Theoretical prediction [$T_{1/2}^{max}$]		
QRPA (Staudt et al)	**= $2.1\cdot10^{22}$**	**= 23 k**
QRPA (Vogel et al)	**= $8.4\cdot10^{20}$**	**= 0.58 M**
NSM (Caurier et al)	**(= $2.1\cdot10^{21}$)**	**(= 0.23 M)**

Sensitivity of ton-scale EXO with barium tagging

Case	Mass (ton)	Eff. (%)	Run Time (yr)	σ_E/E @ 2.5MeV (%)	$2\nu\beta\beta$ Background (events)	$T_{1/2}^{0\nu}$ (yr, 90%CL)	Majorana mass (meV) QRPA[1]	NSM[2]
Conservative	1	70	5	1.6*	0.5 (use 1)	$2*10^{27}$	19	24
Aggressive	10	70	10	1†	0.7 (use 1)	$4.1*10^{28}$	4.3	5.3

1) Simkovic et al. Phys. Rev. C**79**, 055501(2009) [use RQRPA and g_A= 1.25]

2) Menendez et al., Nucl. Phys. A**818**, 139(2009), use UCOM results

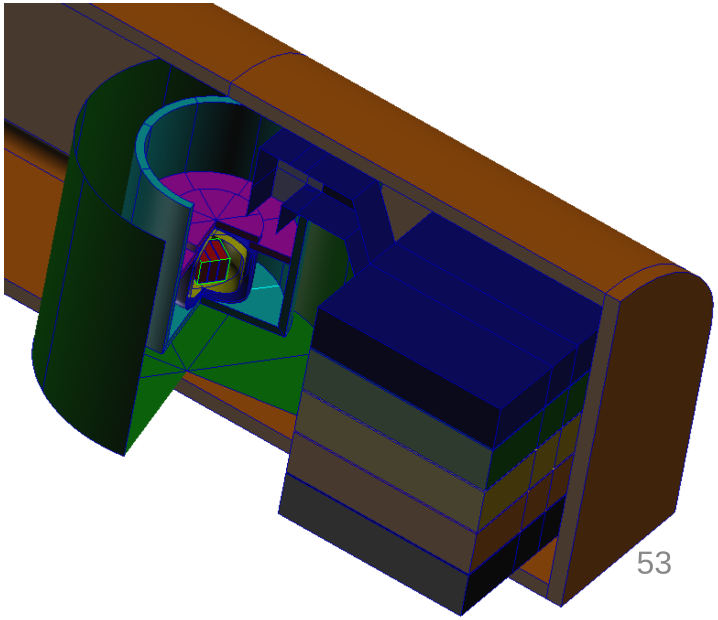

The EXO Collaboration

K. Barry, M. Hughes, R. MacLellan, E. Niner, A. Piepke, K. Pushkin

University of Alabama, Tuscaloosa AL

P. Vogel

California Institute of Technology, Pasadena CA

M. Dixit, K. Graham, C. Green, C. Hagemann, C. Hargrove, E. Rollin, D. Sinclair, V. Strickland

Carleton University, Ottawa ON, Canada

M. Moe

University of California, Irvine, Irvine CA

C. Benitez-Medina, S. Cook, W. Fairbank, Jr., K. Hall, B. Mong

Colorado State University, Fort Collins CO

D. Akimov, I. Alexandrov, A. Burenkov, M. Danilov, A. Dolgolenko, A. Karelin, A. Kovalenko, A. Kuchenkov, V. Stekhanov, O. Zeldovich

ITEP Moscow, Russia

B. Aharmim, K. Donato, J. Farine, D. Hallman, U. Wichoski

Laurentian University, Sudbury ON, Canada

H. Breuer, C. Hall, L.J. Kaufman, D. Leonard, S. Slutsky, Y-R. Yen

University of Maryland, College Park MD

J. Cook, T. Daniels, K. Kumar, P. Morgon, A. Pocar, B. Schmoll, C. Sterpka

University of Massachusetts Amherst, Amherst MA

M. Auger, D. Franco, G. Giroux, R. Gornea, F. Juget, G. Lutter, J-L. Vuilleumier, J-M. Vuilleumier

Laboratory for High Energy Physics, Bern, Switzerland

P.Fierlinger, F.Rosenau

Technical University of Munich, Garching, Germany

N. Ackerman, M. Breidenbach, R. Conley, W. Craddock, S. Herrin, J. Hodgson, D. Mackay, A. Odian, C. Prescott, P. Rowson, K. Skarpaas, M. Swift, J. Wodin, L. Yang, S. Zalog

Stanford Linear Accelerator Center (SLAC), Menlo Park CA

P. Barbeau, L. Bartoszek,, R. DeVoe, M. Dolinski, G. Gratta, M. Green, F. LePort, M. Montero-Diez, A.R. Muller, R. Neilson, K. O'Sullivan, A. Rivas, K. Twelker

Stanford University, Stanford CA